Decentralized adaptive control and system identification, with applications to power systems
by Daniel James Trudnowski

A thesis submitted in partial fulfillment of the requirements for the degree of Doctor of Philosophy in Electrical Engineering
Montana State University

Abstract:
This thesis addresses the problem of damping electromechanical oscillations in power systems using advanced control theory. Two control strategies are developed. Controllers are then applied to a power system as power system stabilizer (PSS) units. The primary strategy is a decentralized indirect adaptive control scheme where multiple self-tuning adaptive controllers are coordinated. This adaptive scheme is developed in a general format and the stabilizing properties are shown using a vector Lyapunov analysis. The second strategy is a new method of designing conventional nonadaptive PSS units. An off-line system identification method based on Prony signal analysis is developed. This Prony identification method and a root-locus technique are used to design the conventional PSS units. Both the adaptive and the conventional strategies are applied to a 17-machine computer-simulated power system. PSS units are applied to four generators in the system. Detailed simulation results are presented that show the feasibility and properties of both control schemes.

DECENTRALIZED ADAPTIVE CONTROL AND SYSTEM IDENTIFICATION, WITH APPLICATIONS TO POWER SYSTEMS

by

Daniel James Trudnowski

A thesis submitted in partial fulfillment
of the requirements for the degree

of

Doctor of Philosophy

in

Electrical Engineering

MONTANA STATE UNIVERSITY
Bozeman, Montana

March 1991

APPROVAL

of a thesis submitted by

Daniel James Trudnowski

This thesis has been read by each member of the thesis committee and has been found to be satisfactory regarding content, English usage, format, citations, bibliographic style, and consistency, and is ready for submission to the College of Graduate Studies.

3/14/91
Date

Donald A. Pierre
Chairperson, Graduate Committee

Approved for the Major Department

3-14-91
Date

Head, Major Department

Approved for the College of Graduate Studies

3/26/91
Date

Henry L. Parsons
Graduate Dean

STATEMENT OF PERMISSION TO USE

In presenting this thesis in partial fulfillment of the requirements for a doctoral degree at Montana State University, I agree that the Library shall make it available to borrowers under rules of the Library. I further agree that copying of this thesis is allowable only for scholarly purposes, consistent with "fair use" as prescribed in the U.S. Copyright Law. Requests for extensive copying or reproduction of this thesis should be referred to University Microfilms International, 300 North Zeeb Road, Ann Arbor, Michigan 48106, to whom I have granted "the exclusive right to reproduce and distribute copies of the dissertation in and from microfilm and the right to reproduce and distribute by abstract in any format."

Signature David T. Trudnowski

Date 3/14/91

ACKNOWLEDGMENTS

I wish to thank my graduate advisor, Dr. Donald Pierre. His guidance, helpful discussions, and constructive criticism throughout my studies and the writing of this thesis have been extremely helpful. I would also like to thank Dr. James Smith for his suggestions and discussions concerning the research. Many others also have been helpful to the work of this thesis including Dr. Iraj Sadighi for allowing me to use his CLS identification software, and Mr. Tom Short for developing a method of integrating controllers in the power-system simulation package.

The financial support of the Electric Power Research Institute, the Bonneville Power Administration, the Montana Electric Power Research Affiliates, and the Montana State Engineering Experiment Station is appreciated.

I would especially like to thank my wife, Diana, for her patience and support throughout my studies. My children, Tony and Jacob, deserve a special thanks because they make the hard work much more rewarding.

Finally, I would like to thank God for giving me the privilege of being associated with the above mentioned people and the many others who have helped me through my graduate studies.

TABLE OF CONTENTS

	Page
LIST OF TABLES	vii
LIST OF FIGURES	viii
NOMENCLATURE	xii
ABSTRACT	xiii
1. INTRODUCTION	1
Power System Electromechanical Oscillations	3
Adaptive Control	7
Decentralized Control	10
Literature Review	17
Conventional Damping Methods using PSS units	18
Adaptive Control in Power Systems	19
Adaptive and Decentralized Control	25
Organization of Thesis	27
2. THE DECENTRALIZED ADAPTIVE CONTROL SCHEME	28
Plant Description	29
The General Control Scheme	34
Identifier	36
Observer	38
Control Law	39
Adaptive Controllers	41
Global Stability	41
Lemma 2.1	42
Proof of Lemma 2.1	43
Lemma 2.2	44
Proof of Lemma 2.2	46
Theorem 2.1	47
Proof of Theorem 2.1	48
Corollary 2.1	51
Proof of Corollary 2.1	52
Remarks on Theorem 2.1 and Corollary 2.1	52
The Specific Control Scheme to be Implemented	53
Properties of the Control Scheme	60
Example 1	60
Example 2	66
Example 3	69
Example 4	72

TABLE OF CONTENTS -- Continued

Page

Example 5 76

3. SYSTEM IDENTIFICATION USING PRONY ANALYSIS 78

Prony Signal Analysis 80
System Identification using Prony Analysis 83
Case 1: Zero Initial Conditions 87
Case 2: Nonzero Initial Conditions 88
Estimating the System Order 90
Choosing the Input 93
Programming the Prony Analysis Method 94
An Example 96

4. IMPLEMENTATION OF CONTROLLERS IN A TEST SYSTEM 99

A 17 Machine Test System 99
Implementation of PSS Units in the Test System 105
Decentralized Adaptive Controllers 110
Criterion for Controller Communication .. 112
Conventional Controllers 115
Embedding Controllers in the Simulation Program ... 124

5. SIMULATION RESULTS 125

Simulations 1 126
Simulations 2 133
Simulations 3 138
Simulations 4 144
Simulations 5 145
Simulations 6 147
Summary of Controller Properties 149

6. CONCLUSIONS AND FUTURE WORK 151

The Decentralized Adaptive Control Strategy 151
Conventional PSS Design and Prony Identification ... 154

REFERENCES CITED 156

APPENDICES 163

A - Adaptive Controller Subroutines 164
B - Prony Identification Software Package 191
C - ETMSP Data Files for the Test System 210
D - PSS Implementation Subroutines 218

LIST OF TABLES

Table		Page
1.	Generation and load of each area (operating point A)	101
2.	Output of each generator (operating point A)	102
3.	Residue magnitudes with input at generator 2	114
4.	Residue magnitudes with input at generator 3	114

LIST OF FIGURES

Figure		Page
1.	Direct adaptive control.....	8
2.	Indirect adaptive control.....	9
3.	Adaptive controller at control station i.....	60
4.	Example 1, open-loop response of y_1.....	63
5.	Example 1, open-loop response of y_2.....	64
6.	Example 1, closed-loop response of y_1.....	64
7.	Example 1, closed-loop response of u_1.....	65
8.	Example 1, closed-loop response of y_2.....	65
9.	Example 1, closed-loop response of u_2.....	66
10.	Example 2, closed-loop response of y_1.....	67
11.	Example 2, closed-loop response of u_1.....	68
12.	Example 2, closed-loop response of y_2.....	68
13.	Example 2, closed-loop response of u_2.....	69
14.	Example 3, closed-loop response of y_1.....	70
15.	Example 3, closed-loop response of u_1.....	71
16.	Example 3, closed-loop response of y_2.....	71
17.	Example 3, closed-loop response of u_2.....	72
18.	Example 4, open-loop response of y_1.....	74
19.	Example 4, open-loop response of y_2.....	74
20.	Example 4, closed-loop response of y_1.....	75
21.	Example 4, closed-loop response of y_2.....	75
22.	System model with initial conditions.....	84

LIST OF FIGURES -- Continued

Figure		Page
23.	$u(t)$ for the case when $\lambda_{n+1}=0$ and $q=3$.....	85
24.	System (3.42) response to the input.....	98
25.	Fitting errors for given model orders.....	98
26.	Test system (operating point A).....	100
27.	Test system (operating point B).....	104
28.	Implementation of a general PSS unit.....	106
29.	An adaptive PSS used in the test system.....	111
30.	A conventional PSS used in the test system..	116
31.	Probing signal and the magnitude of its Fourier transform.....	118
32.	Root-locus plot for generator 4.....	120
33.	Root-locus plot for generator 2.....	123
34.	Root-locus plot for generator 2 (interarea modes).....	123
35.	P_{acc} at generator 2 with adaptive control for Simulations 1.....	127
36.	P_{acc} at generator 3 with adaptive control for Simulations 1.....	127
37.	P_{acc} at generator 2 with adaptive control for Simulations 1 (second controller settings).....	129
38.	P_{acc} at generator 3 with adaptive control for Simulations 1 (second controller settings).....	129
39.	P_{acc} at generator 2 with conventional control for Simulations 1.....	131
40.	P_{acc} at generator 3 with conventional control for Simulations 1.....	131
41.	Generator 2's controlled input for control cases in Simulations 1.....	132

LIST OF FIGURES -- Continued

Figure		Page
42.	Generator 3's controlled input for control cases in Simulations 1.....	132
43.	P_{acc} at generator 2 for adaptive controllers in Simulations 1.....	133
44.	P_{acc} at generator 2 with adaptive control for Simulations 2.....	135
45.	P_{acc} at generator 3 with adaptive control for Simulations 2.....	135
46.	P_{acc} at generator 2 with adaptive control for Simulations 2 (second controller settings).....	136
47.	P_{acc} at generator 3 with adaptive control for Simulations 2 (second controller settings).....	136
48.	P_{acc} at generator 2 with conventional control for Simulations 2.....	137
49.	P_{acc} at generator 3 with conventional control for Simulations 2.....	138
50.	f_{err} at area P with no controllers in Simulations 3.....	140
51.	f_{err} at area P for adaptive control cases in Simulations 3.....	140
52.	f_{err} at area P for adaptive control cases in Simulations 3 (second controller settings).....	142
53.	f_{err} at area P for the conventional control case in Simulations 3.....	142
54.	Generator 2's controlled input for Simulations 3.....	143
55.	Generator 3's controlled input for Simulations 3.....	143
56.	f_{err} at area P in Simulations 4.....	145
57.	P_{acc} at generator 4 for Simulations 5.....	146

LIST OF FIGURES -- Continued

Figure		Page
58.	Controlled inputs at generator 4 for Simulations 5	147
59.	f_{err} in area SC1 for Simulations 6	148
60.	FORTRAN call statement for the CLS subroutine	166
61.	FORTRAN adaptive controller subroutines	167
62.	Running PRONYID	196
63.	PRONYID.OUT for the Chapter 3 example	197
64.	Prony identification programs	198
65.	Loadflow data file for operating point A	212
66.	Loadflow data file for operating point B	214
67.	Swing data file	216
68.	MULTIPLECONT.DAT for the Chapter 4 controllers	220
69.	PSS implementation subroutines	221

NOMENCLATURE

C	Complex number
I^n	n x n identity matrix
$\Re$	Real number
$\Re^n$	n x 1 vector with real entries
$\Re^{n x m}$	n x m matrix with real entries
$\otimes$	Matrix tensor product
$\|x\|$	Euclidean norm of x

ABSTRACT

This thesis addresses the problem of damping electromechanical oscillations in power systems using advanced control theory. Two control strategies are developed. Controllers are then applied to a power system as power system stabilizer (PSS) units. The primary strategy is a decentralized indirect adaptive control scheme where multiple self-tuning adaptive controllers are coordinated. This adaptive scheme is developed in a general format and the stabilizing properties are shown using a vector Lyapunov analysis. The second strategy is a new method of designing conventional nonadaptive PSS units. An off-line system identification method based on Prony signal analysis is developed. This Prony identification method and a root-locus technique are used to design the conventional PSS units. Both the adaptive and the conventional strategies are applied to a 17-machine computer-simulated power system. PSS units are applied to four generators in the system. Detailed simulation results are presented that show the feasibility and properties of both control schemes.

CHAPTER 1

INTRODUCTION

Often in large power systems lightly-damped oscillations, termed electromechanical oscillations, occur due to generators exchanging energy through transmission lines. Many types of unavoidable system disturbances can cause electromechanical oscillations, and severe oscillations can decrease the life of generators and limit the amount of transferable power over transmission lines. Because a power system is a large nonlinear time-varying system, it is often difficult to dampen these oscillations. Conventional methods of damping electromechanical oscillations have proven to be effective in many cases. But, as smaller localized systems are interconnected over large distances, conventional methods of controller design often fail to add adequate damping. In this thesis modern control techniques are applied to this power system problem. The control techniques include adaptive and decentralized control which are very attractive solution methods to this problem. Special attention is paid to the implementation of multiple controllers located throughout the system.

The size and complexity of a power system makes it a candidate for decentralized control methods, while the non-

linear and time-varying properties make the system a candidate for adaptive control. The main objective of this thesis is to present a decentralized adaptive control strategy that may be applied to power systems to dampen electromechanical oscillations. With the strategy, multiple adaptive controllers are coordinated using a decentralized technique. A second objective is to present a nonadaptive design technique for power-system damping controllers. This nonadaptive technique is based on a new system identification method presented in this thesis.

In developing the damping controllers in this thesis, emphasis is placed on the practicality of being able to apply them to an actual system. The control schemes are designed so that the control action at a given control station has minimal dependence on variables which cannot be measured locally. In this way the control scheme will not be highly dependent on communication between different locations in the network. Nondependence on communication is important as the same factors that cause electromechanical oscillations can also cause communication failures.

Because power systems are often difficult to accurately model, it is desired that the design of the controllers have minimal dependence on computer simulation of the system. Although the control schemes in this thesis are demonstrated on a computer-simulated system, the controllers

are developed with the idea of being able to apply them to an actual system without dependence on computer models or simulations.

The remaining material of this chapter is organized into five sections. A description of the problem being addressed is given in the first section. Adaptive and decentralized control concepts are introduced in the second and third sections. A literature review of recent published work is contained in section four. In the last section the organization of the remaining thesis is outlined.

Power System Electromechanical Oscillations

In a power system, turbines are used to rotate the rotors of large synchronous generators. The generators then convert this rotational energy into electrical energy. In order to connect several generators together to form a power system, the machines must rotate on average at the same constant speed. In modern systems this synchronous speed relates to the electrical frequency of 50 or 60 Hz. Because the rotor of a synchronous generator is a large rotating mass, it must obey the laws of nature. When a sudden disturbance occurs in the system, the circuit laws of Kirchhoff force the electrical power from a synchronous generator to suddenly change, while the mechanical power into the generator has not changed. This imbalance of

power causes the rotor to suddenly accelerate or decelerate away from synchronous speed initiating the electromechanical oscillations. If the generator cannot return to synchronous speed, it is said to have separated from the system. As generator rotors accelerate and decelerate energy is oscillated through the system. Because of the laws of conservation of energy, this energy is absorbed by loads and by other generators which causes various generators to "swing against one another." Generators that swing against one another oscillate 180° out of phase.

Most often electromechanical oscillations occur in the 0.2 to 3.0 Hz range with these frequencies being a function of many variables including rotor inertias. These oscillations can be initiated by a variety of "sudden" disturbances in the system, such as a transmission line fault. An electromechanical oscillation in a power system is often termed a system swing. Significant system swings can be detrimental to the power system. If the oscillations are negatively damped, then the system will separate during a swing which can cause significant damage to utility and customer equipment. If system swings are only lightly damped, then a combination of disturbances may cause the system to swing past its steady-state limits which can also cause system separation. In any case, it is important to add significant damping to power-system electromechanical oscillations in order to preserve system integrity.

Electromechanical oscillations are often considered to be of two types: local and interarea. A local mode of oscillation occurs when a single generator swings against the system. These modes tend to be localized near the given generator and are generally in the 0.8 to 3.0 Hz range. Interarea modes occur when a group of generators swing together against other groups of machines. Because interarea modes involve multiple machines (which implies more mass), they tend to be at lower frequencies than local modes. The range of frequencies for interarea modes are generally between 0.2 Hz and 0.8 Hz. Usually, interarea modes occur between groups that are weakly connected and are often the most troublesome modes in large systems.

Recent advancement of technology in the power industry has caused electromechanical oscillations to become more prevalent in many systems (especially interarea modes) [1]. With smaller faster-reacting generators being developed, it takes less energy to force a given generator to swing. Also, many systems are being operated near their steady-state limits with larger amounts of power being transferred greater distances which tends to increase the electromechanical oscillation problem. In many cases, conventional controllers are unable to adequately dampen these oscillations, especially interarea modes. Therefore, there is a need for more effective solutions for adding damping to power systems.

Various devices have been proposed to dampen electromechanical oscillations including power system stabilizer (PSS) units, static volt-amp-reactive compensators (SVC's), and modulation of high-voltage DC (HVDC) converter systems. Of these, PSS units have received the majority of attention and have proven to be successful in some cases. PSS units are feedback circuits applied to the excitation system of a synchronous generator. SVC's are variable reactive devices that are primarily used for voltage support; although, they have proven to be effective as a damping device as well. Modulation of HVDC systems involves varying the converter firing angle about a nominal point in order to modulate the power flow on the DC line.

The control schemes in this thesis are presented in a general format so that they may be applied to many different types of systems. When applied to the power system for simulation results, the schemes are implemented using PSS units. PSS units are used because this is the most widely used damping device in the power industry. It is believed that if a new control technique (such as those proposed in this thesis) is used by the industry, it will first be tried on a PSS unit.

The operating point of a power system changes both seasonally and hourly as loads change. With each different operating point the dynamics of the system change. This time-varying nature of the system makes it difficult and

sometimes impossible to design a conventional controller that will satisfactorily dampen oscillations at each operating point. Obtaining system models for controller design using the laws of physics is often very difficult because of the size and complexity of power systems. Both the adaptive and the nonadaptive control methods presented in this thesis are based on system identification methods that result in system models by analyzing signals from the actual system.

Adaptive Control

Adaptive control is an area of feedback control theory that has recently received a great deal of attention. Although there is no clear-cut definition of adaptive control, an adaptive controller may be viewed as a regulator that can modify its behavior according to changes in the dynamics of the process it is controlling [2]. Conventional adaptive controllers have a self-learning ability in that the designer does not have to know a great deal about the plant that is to be controlled. The adaptive controller "learns" about the plant by analyzing its input/output relationship. The controller adjusts its feedback parameters as it learns about the plant or as the plant changes.

The learning ability of adaptive control makes it very attractive for application to the power system problem. It

is often extremely difficult to obtain an accurate mathematical model of a power system. This is because a power system is a nonlinear time-varying system of very large order; the time-varying properties of the system are both stochastic and nonstochastic.

Adaptive controllers are generally broken into two different types: direct and indirect [2]. With the direct adaptive controller, regulator parameters are directly changed as the dynamics of the system change. This is demonstrated in Figure 1. The closed-loop plant is forced to act like a model system; the regulator parameters are adjusted until the error e in Figure 1 is driven to zero. Direct adaptive control is often termed model-reference adaptive control (MRAC).

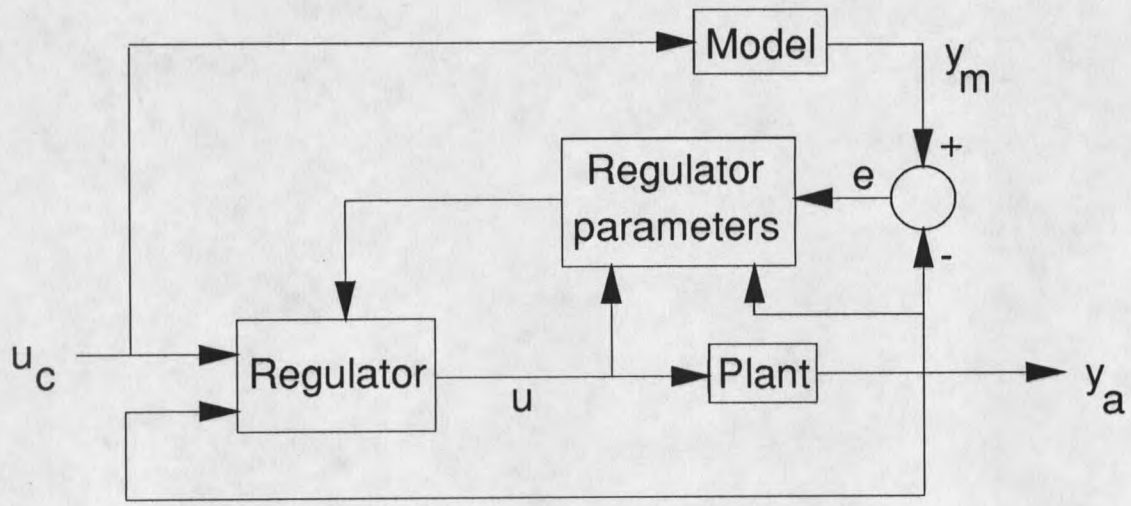

Figure 1. Direct adaptive control.

With an indirect adaptive controller the regulator parameters are indirectly updated; an indirect controller is shown in Figure 2. The controller's operation occurs in two distinct steps. First, the dynamics of the system are identified at a particular instant in time; then the regulator is adjusted according to the identified dynamics. The plant's input and output are passed to a recursive identifier which identifies a linear model of the plant. The linear model parameters are passed to a regulator design block. Here the regulator parameters are calculated and passed to the regulator. With a discrete-time adaptive controller, the whole process may be updated with each time sample. Indirect adaptive controllers are also termed self-tuning adaptive controllers.

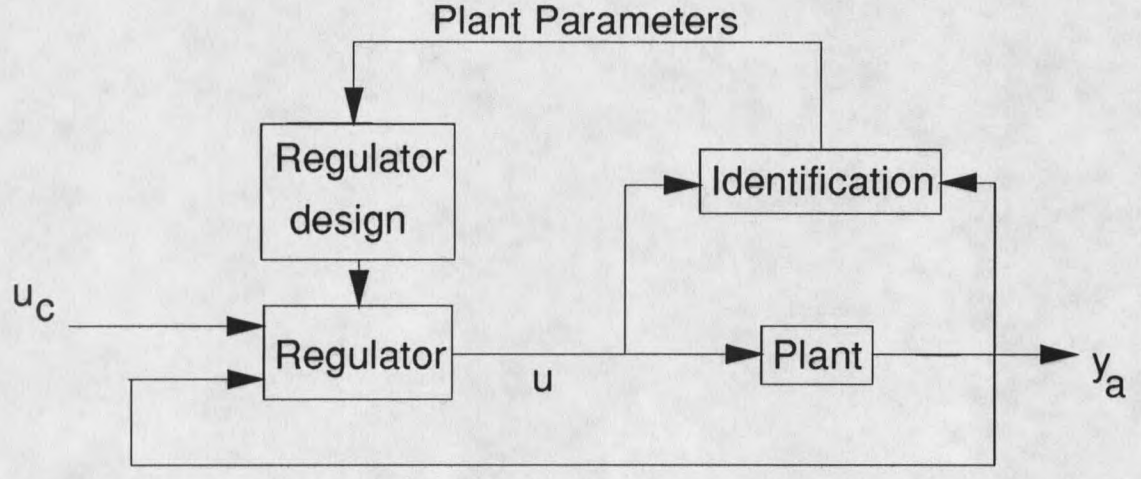

Figure 2. Indirect adaptive control.

A direct adaptive controller is not well suited for the power system problem because a reference model must be cho-

sen for the closed-loop system. Since a power system is a time-varying plant, a reference model adequate at one point in time may not be adequate at other times. Also, it is difficult to obtain direct criteria for choosing a reference model. Therefore, the adaptive controller strategy presented in this thesis is an indirect type.

An important issue concerning an indirect adaptive controller is the choice of the regulator design algorithm. The objective of the controller is to dampen electromechanical oscillations as well as possible, given an allowable range of input. A pole-placement algorithm is ruled out as this requires a choice of closed-loop poles which can be difficult for a time-varying plant. A regulator based on a linear-quadratic (LQ) control law is a good candidate because it can be used to directly penalize swings in the system while at the same time limiting action in the controlled input. An LQ controller is easily placed in a recursive form using Riccati equations; this makes it easy to implement such a controller in an adaptive format. For these reasons the adaptive control strategy in this thesis is based on an LQ control law.

Decentralized Control

Many systems exist with multiple locations in the plant where input signals can be applied; these plants are often referred to as multiple control-station systems. Various

options are available when considering the control of a multiple control-station system. For the power system problem it is desired that the control action at a given station have minimal dependence on variables which cannot be measured locally. In this way the control scheme will not be dependent on communication between different locations in the network. Nondependence on communication is important as the same factors that cause electromechanical oscillations can also cause communication failures. If communication is used, it is desired that the controllers still effectively operate when communication fails. This requirement points to a decentralized control solution.

With a decentralized scheme, controllers are applied at each control station with a central objective. The controller at a given station is designed to be primarily dependent on local measurable variables. Therefore, if communication of variables from outside sources fails, the controller can still properly operate. A second advantage of decentralized control strategies is that the failure of one controller has no detrimental effect on the performance of other controllers. There are two basic classes of decentralized control. The first class is often termed sequential control. For lack of a better term, the second class is referred to in this thesis as the nonsequential class.

With a sequential scheme the controller designs at the control stations are carried out sequentially one-by-one. Consider a plant consisting of m control stations. First a model of the system is obtained from the input to the output at station 1 while ignoring the inputs at other stations. A controller is designed for station 1 using this model, and the controller is applied to the plant. Then a model of the system is obtained from the input to the output at station 2, and the controller is designed and applied. The sequential process continues for all m control stations. If the objective of the controller at each station is the same, then this objective will be fulfilled in the end if certain observability and controllability conditions are satisfied. As an example, in [3] the objective for each controller design is to place the closed-loop poles in a certain specified region (Γ_s). Davison and Ozuguner [3] show that after the sequential design, all of the closed-loop poles are contained in Γ_s.

The sequential technique is not easily applicable to the case where the controller at each station is an adaptive one. This is because the sequential technique requires that when a given controller is designed, all previously designed controllers be fixed and applied to the system. An adaptive controller is constantly changing as the system changes; therefore, it would not be fixed when designing other controllers. Although the sequential

method does not apply well to the adaptive case, it does apply well to the nonadaptive case where the controllers are fixed. A sequential method is used to implement multiple fixed damping controllers for a simulated power system later in this thesis.

Nonsequential decentralized controller design techniques assume the system is broken into a number of interconnected subsystems. With most designs, a local controller is designed for each subsystem while ignoring the subsystem interconnections. Then modifications are made to the designs to help negate any detrimental effect of the subsystem interconnections. Because the subsystem interconnections are ignored during the initial designs, the performance of the controllers are very robust to changes in subsystem interconnections. Also, since the designs of the controllers are independent, failure of one controller will have no detrimental effect on the performance of other controllers.

Characteristics of a nonsequential design are easily shown using the following example from [4]. Consider a system consisting of two subsystems. The state-space differential equations describing the system are

$$\dot{x}_1 = 5x_1 + (-3x_2) + u_1 \tag{1.1a}$$

$$\dot{x}_2 = 6x_2 + (-4x_1) + u_2 \tag{1.1b}$$

where u_1 is the input and x_1 is the output at subsystem 1; u_2 is the input and x_2 is the output at subsystem 2; and the terms in (•) are the subsystem interconnections.

First, let the control functions u_1 and u_2 be chosen in a centralized fashion by minimizing the standard LQ cost function

$$J = \int_0^\infty (x_1^2 + x_2^2 + u_1^2 + u_2^2)dt \tag{1.2}$$

In this case it is easy to show [5] that the optimal feedback functions are

$$u_1 = -10.49x_1 + 7.14x_2 \tag{1.3}$$
$$u_2 = 7.14x_1 - 11.18x_2$$

and the closed-loop eigenvalues are -8.9, -1.7. Now what happens if the subsystem interconnections are lost so that the plant becomes

$$\dot{x}_1 = 5x_1 + (-0x_2) + u_1 \tag{1.4a}$$

$$\dot{x}_2 = 6x_2 + (-0x_1) + u_2 \tag{1.4b}$$

The closed-loop system of the perturbed plant (1.4) and control law (1.3) is an unstable system with eigenvalues at -12.5 and 1.8. Therefore, the centralized control law of (1.3) is not robust to these changes in the subsystem interconnections.

Now, consider a nonsequential decentralized design for the system (1.1). The subsystem interconnections are ignored resulting in the two subsystems

$$\dot{x}_1 = 5x_1 + u_1 \tag{1.5a}$$

$$\dot{x}_2 = 6x_2 + u_2 \tag{1.5b}$$

and the cost function is broken into two functions:

$$J_1 = \int_0^\infty (x_1^2 + u_1^2)dt \tag{1.6a}$$

$$J_2 = \int_0^\infty (x_2^2 + u_2^2)dt \tag{1.6b}$$

A feedback function is found for subsystem 1 by obtaining the control law that minimizes (1.6a) for (1.5a); the same is done for subsystem 2. The resulting control laws are

$$u_1 = -10.10x_1, \quad u_2 = -12.05x_2 \tag{1.7}$$

In order to negate the effects of the subsystem interconnections, the control laws of (1.7) are modified to

$$u_1 = -10.10x_1 + 3x_2 \tag{1.8}$$

$$u_2 = -12.05x_2 + 4x_1$$

The closed-loop eigenvalues of the plant (1.1) and the control law (1.8) are -5.10 and -6.05. Again, consider the perturb plant (1.4), but now use the control law of (1.8). In this case the closed-loop eigenvalues are -2.1 and -9.1; therefore, the system is stable.

One does not have to modify the control law (1.7) to (1.8). The law (1.7) applied to the plants (1.1) and (1.4) also results in stable systems, and in this case the control functions at each subsystem are only a function of local variables. So why modify the feedback functions?

Modifying (1.7) to (1.8) negates any effect of the subsystem interconnections in the nominal plant case. The controllers were designed by ignoring the interconnections; therefore, modifying the control law to negate the interconnections results in the closed-loop system satisfying the design objective. For the above example, the design objective is to obtain the closed-loop system where the cost functions (1.6) are minimized for systems (1.5). Since the systems in (1.5) do not incorporate the interconnections, the control laws are modified to negate the effects of the interconnections.

The above example demonstrates that a nonsequential decentralized design can improve system robustness to perturbations in the interconnections. Decentralized controllers have other advantages. With a centralized controller, the control laws require communication between subsystems. For the above example u_i in (1.3) is a function of both x_1 and x_2. If communication fails between subsystems, then the control law is not valid and the results can be catastrophic. Any communication used with a decentralized control law is a modification to the original law. Therefore, if communication fails, the controllers still strives to fulfill the control objective. Another advantage of a decentralized design involves the failure of a given controller. If the control law at a subsystem fails for some reason, the remaining control actions at other subsystems

still apply the proper input to the system. This is because the control law at each subsystem is designed separately from other controllers. In the centralized case all control laws are designed together; therefore, if one control law fails, all laws may fail.

It is possible to use a nonsequential design method when the controllers used at each subsystem are adaptive. With an indirect adaptive controller at a given subsystem the identifier has to obtain a model for that subsystem. The regulator design is based on that identified subsystem model. Modification could be done to account for the effects of the subsystem interconnections. This is the strategy used to develop the decentralized adaptive controller presented in Chapter 2. Adaptive controllers are applied at each station of a multistation system. The controllers are designed to control the subsystems connected to that station. Information that enhances the performance of the controllers is communicated between stations. The performance of the control scheme is improved using communication, but in many cases the controllers still properly operate if communication is lost because the design is based on a decentralized technique.

Literature Review

The purpose of this section is to review some of the literature relevant to issues addressed in this thesis.

Thousands of papers have been published in the areas of power system stability, adaptive control, and decentralized control. It would be very cumbersome to review all literature in these areas. Therefore, an attempt is made here to only review recent work that has direct relevance to the subjects contained in this thesis. The remainder of this section is organized into three parts with the following subjects reviewed: 1) conventional damping methods; 2) adaptive control in power systems; and 3) adaptive and decentralized control.

Conventional Damping Methods using PSS Units

The most widely used electromechanical damping device is the PSS unit. The heart of the conventional PSS unit consists of a low-pass wash-out filter and a series of lead-lag blocks. Filtering is used to remove any DC and high-frequency components from the feedback signal, and the lead-lag is used for the control compensation. Choosing the parameters for the PSS unit is termed "tuning." A classical set of papers on tuning PSS units by Larson and Swann is contained in [6]. Many of the concepts used in [6] were first introduced by de Mello and Concordia in [7]. The basic concept involves producing an electrical torque on the machine being controlled that is in phase with the speed error of the machine. Therefore, when the machine is speeding up, the electrical torque tends to slow the

machine, and vice versa. Frequency response methods are used to obtain the PSS parameters that give the proper phase correction.

This classical design method has proven to work very well in many cases, and there have been many extensions of this method, e.g. see [8]-[12]. Detailed computer modeling and system eigenvalue analysis have been used in conjunction with frequency response methods (see [8]-[10] and [12]).

An alternative to obtaining an electrical torque component is to consider the machine as a general system with the input added to the exciter and the output being the chosen feedback signal. This is the approach taken by Bollinger and Chapin in [13]. In [13] a pseudo random signal is applied to the exciter in the open-loop case. A frequency response of the machine is obtained, and a linear transfer-function model is derived from the frequency response. It is not mentioned how the transfer function is derived. A root-locus design method is used to select the PSS parameters. This is done by making the eigenvalues associated with the electromechanical modes move farther into the left-hand plane.

Adaptive Control in Power Systems

Because adaptive control is an attractive solution for damping electromechanical oscillations, it has received a significant amount of attention in the literature. In [14]

Pierre gives a perspective on the status of adaptive control in power systems as of 1987. A number of papers published before 1987 are reviewed. Eight of the nine papers reviewed for the electromechanical problem use self-tuning adaptive control as opposed to model-reference adaptive control. In each of these nine papers the adaptive controller is implemented as a PSS unit on a single generator; none of them include multiple adaptive controllers. Five of the self-tuners are based on regulator algorithms that do not guarantee stability in the nonminimum-phase case. This can be a problem in a power system as the linearized plant is often nonminimum phase. All of these papers conclude that their adaptive controller is superior to a fixed controller. But, the test systems in many of these papers are overly simplified.

Since 1987 research has continued on applying adaptive control to power systems. Smith, et al., apply an LQ self-tuning adaptive controller to an SVC to control the susceptance of the compensator in [15]. The LQ cost function includes a penalty on the rate-of-change of the adaptive output signal (the susceptance). This allows the designer to temper the rate-of-change of the control action. Simulation results that demonstrate the damping ability of the controller are shown on a three-machine system. The authors of [15] expand their work in [16] to include a secondary proportional-integral (PI) loop in the control-

ler. The conventional PI controller is used to force the steady-state voltage at the SVC bus to the set point. The LQ adaptive controller is used to modulate the SVC susceptance about the set point to dampen system oscillations. In both [15] and [16] electrical frequency error is used as the input to the adaptive controller, and in [16] the bus voltage is also used as an input to the controller. Also, recursive least-squares (RLS) identification is used to obtain a model of the system in the self tuner. Model orders are assumed to be third or fifth.

A self-tuning LQ controller is also used by Mao, et al., in [17]. The controller is used as a PSS unit. No penalty is included on the rate-of-change of the control action as in [15] and [16]. The feedback signal is a linear combination of terminal voltage and frequency error. Simulation results are shown for a one-machine and a three-machine system. In the three-machine case, all machines are equipped with adaptive controllers, but no coordination is used between controllers. The simulations demonstrate that the controllers add damping to the system. The authors of [17] apply their adaptive PSS unit to a laboratory machine in [18]. The machine is a 3 kVA, 210 V, three-phase micro-alternator. Simulations show that the adaptive PSS unit adds significant damping to the system.

In [19] Short, et al., use adaptive control to modulate a switched capacitor bank to obtain system damping. A form

of self-tuning generalized predictive control (GPC) with discrete constraints placed on the control signal is used. An RLS identifier is used to obtain a model of the power system. GPC is a generalization of LQ control. With GPC system outputs are predicted over a specified horizon for each possible control action. The chosen control action is the one that minimizes a weighted-squares cost function of terms that include local system outputs and rate-of-change of control over the horizon. Simulation results are shown on the same three-machine system used in [15] and [16]. Good results are shown using frequency error, integrated frequency error, and bus voltage angle as feedback signals.

Pahalawaththa, et al., in [20], Gu and Bollinger in [21], and Wu and Hogg in [22] use a generalized minimum variance (GMV) control law as the regulator in a self-tuner. In these three papers the controller is implemented as a PSS unit on a one-machine infinite-bus system. Although minimum-variance algorithms are known to have trouble stabilizing nonminimum-phase plants, the authors in [20] claim that a GMV controller can stabilize such plants. RLS identification is used in these papers, and it is assumed that the plant is third order. The RLS algorithms in [20] and [21] use a variable forgetting factor. In [22] an extensive supervision scheme is outlined. The sampling period used in [20] is 100 ms, 50 ms in [21], and 20 ms in [22]. The results shown in these papers demonstrate that a

GMV self tuner can dampen system oscillations for various operating conditions. In [21] comparisons are made with a standard PSS unit. Bollinger and Gu extend their work in [23] by comparing the GMV self-tuner to a standard PSS design for a single machine in a nine-machine system. They conclude that the adaptive controller adds more damping to the system. Dash, et al., also use a minimum-variance regulator as a basis for a self-tuner used to control an SVC unit in [24].

In [25] Fan, et al., develop a multi-input self-tuning adaptive PSS unit. The controller is based on a GMV control law as in [20]-[23], and an RLS identifier with a variable forgetting factor is used as the identifier. A unique contribution of the technique in [25] is that a multi-input identification model is used. The extra inputs to the identifier are represented as system exogenous inputs. Terminal voltage magnitudes are used as these inputs. A multi-rate sampling scheme is used with the identifier model being updated every other sample. Simulation results are shown on a ten-machine system with various machines equipped with adaptive PSS units. These results indicate that the control scheme provides very good damping to the system.

The self-tuning PSS unit presented in [26] by Cheng, et al., uses a self-searching pole-shifting control technique as the regulator part of the adaptive controller. With the

pole-shifting algorithm, the feedback function is determined by shifting the open-loop poles inward toward the origin by a specified factor (in the Z domain). The shifting factor is adjusted so that the poles are moved as much as possible for a given amount of allowable control action. With each time sample, the factor is updated. An RLS identifier with a variable forgetting factor is used to obtain the system model. Extensive simulation results are presented for a one-machine infinite-bus system. In [27] Chandra, et al., also use a pole shifting algorithm; but, the feedback function in [27] is also made to minimize a variance involving past inputs and outputs. That is, the control law minimizes a variance cost function constrained by having the poles shifted radially inward. The authors apply the controller to all machines in a three-machine system. With the results shown the control algorithm performs very well.

A MRAC scheme is used by Ghandakly and Idowu in [28]. The controller is used to generate a modulating signal to both the exciter and the governor of a generating unit. The generating unit's output variables are forced to follow those of a reference model. This reference model consists of two submodels; one corresponding to the machine and exciter; and one corresponding to the governor. The controller is applied to a one-machine infinite-bus system with good damping results.

Adaptive and Decentralized Control

There are numerous books and papers on adaptive and decentralized control techniques. Astrom and Wittenmark's book [2] is a good source of up-to-date adaptive control methods. Siljak's book [4] on large-scale systems contains a good introduction to decentralized control while a more complete and rigorous presentation is done by Michel and Miller in [29]. Both of these books address nonsequential decentralized control techniques. Less literature is available on the combination of adaptive and decentralized control. Although there is a significant number of papers on decentralized MRAC techniques, there are only a few papers available on decentralized self-tuning control. All these papers use nonsequential decentralized control methods to incorporate multiple adaptive controllers.

In [30] Ossman uses self-tuning adaptive controllers at each control station of a multistation plant. The controllers are based on an LQ control law and a gradient identification algorithm. A dead zone is used in the system identification algorithm at each station. By incorporating this dead zone, accurate system identification is possible and global stability can be achieved. Control actions and measured plant outputs must be communicated between stations in order to implement the control strategy.

A decentralized self-tuning control scheme is also presented in [31] by Datta and Ioannou. The control scheme

is different from many others in the literature as it is a continuous-time one. Two different control laws on which to base the self-tuner are proposed, one is pole-placement, and the other is an LQ law. The measured outputs at the control stations are communicated between stations and are used by the continuous-time identifiers. By using this information, global stability limits are obtained.

A small sample of recent papers addressing the decentralized direct adaptive control problem is contained in [32]-[34]. With these methods MRAC type controllers are applied to each station. The MRAC schemes are modified so as to guarantee overall system stability assuming the subsystem interconnections satisfy given conditions. Often global stability limits are obtained without the use of communication between control stations.

A very attractive adaptive controller is presented by Samson and Fuchs in [35]. The controller is a self tuner based on an LQ control law and any identifier that satisfies some general properties (such as RLS). State feedback is used to form the controlled input; an adaptive observer is used to estimate the states. Samson and Fuchs show that the adaptive controller stabilizes both minimum and nonminimum-phase systems. No work is done in [35] to include more than one controller in a decentralized format.

Organization of Thesis

The remainder of this thesis consists of five chapters. In Chapter 2 a decentralized adaptive indirect control scheme is developed. The stabilizing properties of the scheme are given, and examples are used to demonstrate properties of the controller. An off-line system identification method is presented in Chapter 3. The method is based on Prony signal analysis. In Chapter 4 a power system test bed is described, and also discussed is how controllers are implemented in the test system. Two different control schemes are implemented, one uses the decentralized adaptive controller described in Chapter 2, and the other is a conventional scheme based on the system identification method of Chapter 3. Simulation results are given in Chapter 5, and conclusions are made in Chapter 6.

CHAPTER 2

THE DECENTRALIZED ADAPTIVE CONTROL SCHEME

In this chapter the discrete-time decentralized indirect adaptive control scheme that is applied to the power system problem in later chapters is presented. The control scheme is first introduced in a general format that allows a number of variations. Stabilizing properties and proofs of these properties are presented in a concise mathematical format. Then the specific decentralized adaptive scheme that is applied to a power system in later chapters is given. This specific scheme is a special case of the general one. The decentralized adaptive control scheme is presented assuming the plant is a general linear dynamic interconnected system. Examples are used to demonstrate the properties of the control scheme.

The decentralized indirect adaptive control scheme presented here is a discrete-time scheme in which indirect adaptive controllers are applied to each control station of a multi-control-station plant. The adaptive controller applied at a given control station consists of an identifier, a control law, and an observer. A recursive identification algorithm is used to obtain a model of the subsystems "seen" by that control station, and a state-space

linear-quadratic (LQ) control strategy based on the "seen" subsystems is used to form the controlled input. A decentralized observer is used at each station to estimate subsystem states for the LQ feedback gains. When needed, control actions are communicated so that the identifiers can accurately model the subsystems in the presence of their interconnections. The communicated control actions are also used by the decentralized observers to give accurate estimates of subsystem states in the presence of subsystem interconnections. It is shown in this chapter that using the communicated control actions in the observer design at each control station significantly improves system global stability limits.

This chapter contains five main sections with the following items addressed: 1) a description of the plant; 2) the general decentralized adaptive control scheme; 3) stabilizing properties of the control scheme; 4) the specific control scheme to be implemented; and 5) properties of the control scheme (including illustrative examples). Throughout this chapter the variable t represents discrete-time.

Plant Description

Many dynamic plants consist of a number of interconnected subsystems that can be controlled from control stations located in the plant. These plants are often

referred to as interconnected systems. In a general setting, given subsystems can be shared between different control stations with the number of subsystems greater than the number of control stations. In this case the system is referred to as an overlapping interconnected system ([36] and [37]).

A power system, for example, can be viewed as an overlapping interconnected system. A single generator will typically oscillate at both local and interarea modes. Consider the PSS inputs at given generators as the control stations, and let the electromechanical modes be the subsystems. Because an interarea mode involves many generators, it may be viewed as being shared among the PSS inputs at these generators. This motivates the use of an overlapping plant description for derivation of the decentralized adaptive control scheme.

Consider the general linear time-invariant interconnected plant with m subsystems and N control stations

$$\bar{x}_i(t+1) = \bar{A}_i \bar{x}_i(t) + \sum_{j=1}^{N} \bar{b}_{ij} u_j(t) \quad ; \quad i = 1,2,\ldots,m \tag{2.1a}$$

$$y_j(t) = \sum_{i=1}^{m} \bar{c}_{ji}^T \bar{x}_i(t) \quad ; \quad j = 1,2,\ldots,N$$

where $\bar{x}_i(t) \in \Re^{\bar{n}_i}$ is the ith state vector at discrete-time t, $u_i \in \Re$ and $y_i \in \Re$ are the scalar input/output pair at control station i, and $\bar{A}_i \in \Re^{\bar{n}_i \times \bar{n}_i}$, $\bar{b}_{ij} \in \Re^{\bar{n}_i}$, $\bar{c}_{ji} \in \Re^{\bar{n}_i}$. When $m > N$, (2.1a) is termed an overlapping interconnected system as some of

the subsystems are shared among different control stations (see [36] and [37]). Equations (2.1a) may also be written as

$$\bar{x}(t+1) = \bar{A}\bar{x}(t) + \bar{B}u(t) \qquad (2.1b)$$
$$y(t) = \bar{C}\bar{x}(t)$$

where $\bar{x}^T(t) \equiv [\bar{x}_1^T(t), \bar{x}_2^T(t), \ldots, \bar{x}_m^T(t)]$, $u^T(t) \equiv [u_1(t), u_2(t), \ldots, u_N(t)]$,

$y^T(t) \equiv [y_1(t), y_2(t), \ldots, y_N(t)]$,

$$\bar{A} \equiv \text{block diag}(\bar{A}_i), \quad i = 1, 2, \ldots, m$$

$$\bar{B} \equiv \begin{bmatrix} \bar{b}_{11} & \bar{b}_{12} & \cdots & \bar{b}_{1N} \\ \bar{b}_{21} & \bar{b}_{22} & \cdots & \bar{b}_{2N} \\ \cdot & \cdot & & \cdot \\ \cdot & \cdot & & \cdot \\ \cdot & \cdot & & \cdot \\ \bar{b}_{m1} & \bar{b}_{m2} & \cdots & \bar{b}_{mN} \end{bmatrix}, \quad \bar{C} \equiv \begin{bmatrix} \bar{c}_{11}^T & \bar{c}_{12}^T & \cdots & \bar{c}_{1m}^T \\ \bar{c}_{21}^T & \bar{c}_{22}^T & \cdots & \bar{c}_{2m}^T \\ \cdot & \cdot & & \cdot \\ \cdot & \cdot & & \cdot \\ \cdot & \cdot & & \cdot \\ \bar{c}_{N1}^T & \bar{c}_{N2}^T & \cdots & \bar{c}_{Nm}^T \end{bmatrix}$$

and $\bar{A} \in \Re^{\bar{n}x\bar{n}}$, $\bar{B} \in \Re^{\bar{n}xN}$, $\bar{C} \in \Re^{Nx\bar{n}}$ with $\bar{n} = \bar{n}_1 + \bar{n}_2 + \ldots + \bar{n}_m$.

It is shown in [36] that a system can be expanded through a set of linear transformations to a larger dimension using the inclusion principle. The expanded system can be made to have the same input/output characteristics as the original system (termed the contracted system). If $\bar{x} \in \Re^{\bar{n}}$ and $x \in \Re^n$ are the state vectors of a contracted and expanded representation of a system, respectively, with $\bar{n} \leq n$, then they are related through the transformations $x = V\bar{x}$ and $\bar{x} = Ux$ where $V \in \Re^{nx\bar{n}}$ is a constant matrix with full

column rank, $U \in \Re^{\bar{n}xn}$ is a constant matrix with full row rank, and these transformation matrices satisfy the condition $UV = I^{\bar{n}}$.

The plant (2.1) is now expanded into a form that allows the application of decentralized indirect adaptive controllers. Let $V \in \Re^{nx\bar{n}}$ and $U \in \Re^{\bar{n}xn}$ be the smallest transformation matrices in dimension n (with $\bar{n} \leq n$) that expands (2.1b) through the transformations $x = V\bar{x}$ and $\bar{x} = Ux$ to

$$x(t+1) = Ax(t) + Bu(t) \qquad (2.2a)$$
$$y(t) = Cx(t)$$

where u and y are the same as in (2.1b), and

$x^T(t) \equiv [x_1^T(t), x_2^T(t), \ldots, x_N^T(t)]$,

$$A \equiv \text{block diag}(A_i), \quad i = 1,2,\ldots,N$$

$$B \equiv \begin{bmatrix} b_{11} & b_{12} & \ldots & b_{1N} \\ b_{21} & b_{22} & \ldots & b_{2N} \\ \cdot & \cdot & & \cdot \\ \cdot & \cdot & & \cdot \\ \cdot & \cdot & & \cdot \\ b_{N1} & b_{N2} & \ldots & b_{NN} \end{bmatrix}, \quad C \equiv \begin{bmatrix} c_1^T & 0 & \ldots & 0 \\ 0 & c_2^T & \ldots & 0 \\ \cdot & \cdot & & \cdot \\ \cdot & \cdot & & \cdot \\ \cdot & \cdot & & \cdot \\ 0 & 0 & \ldots & c_N^T \end{bmatrix}$$

and $A_i \in \Re^{n_i x n_i}$, $b_{ij} \in \Re^{n_i}$, $c_i \in \Re^{n_i}$. Systems (2.2a) and (2.1b) are related by $A = V\bar{A}U$, $B = V\bar{B}$, and $C = \bar{C}U$. Note that (2.2a) does not allow any subsystems to overlap between control stations; that is, U and V are a pair of matrices that transform an overlapping system into a non-overlapping system. Equations (2.2a) can also be written as

$$x_i(t+1) = A_i x_i(t) + b_{ii} u_i(t) + \sum_{j=1, j\neq i}^{N} b_{ij} u_j(t) \qquad (2.2b)$$

$$y_i(t) = c_i^T x_i(t) \quad ; \quad i = 1,2,\ldots,N$$

where $x_i \in \Re^{n_i}$. Equations (2.2b) represents the plant as N interconnected subsystems (one for each control station) with the b_{ij} terms being the interconnection terms. The above transformation alters the plant representation so that the interconnection terms only involve the plant inputs and not the outputs. Because (2.2) is an expansion of (2.1), the inclusion principle asserts that (2.2) contains all necessary information about (2.1) (see [37]).

Since the expanded system (2.2) preserves the input/output characteristics of (2.1), any input that stabilizes (2.2) will also stabilize (2.1) (see [37] for a proof). That is, if the decentralized stabilizing feedback control function

$$u_i(t) = f_i(x_i(t)); \quad i = 1,2,\ldots,N \qquad (2.3)$$

is designed for the expanded plant representation (2.2) and the exact same u_i's of (2.3) are applied to (2.1), then (2.1) will also be stabilized. Also, the closed-loop system of (2.2) and (2.3) will be an expansion of the system with (2.3) applied to (2.1); therefore, the two will have the same closed-loop input/output characteristics.

This is the basis for the decentralized indirect adaptive controller presented in this thesis. The plant is

identified in the expanded form of (2.2b) using an identification scheme, and a decentralized adaptive control law is designed using the expanded form. Then the controlled input is applied to the actual plant (2.1). The inclusion principle assures that the application of this control law will result in the desired stability and input/output closed-loop characteristics.

In order to implement the decentralized adaptive control strategy in this paper, the U and V transformation matrices need not be known. All that must be known about the system is the dimension of the expanded subsystems in (2.2b); that is, the n_i's. This is not an overly restrictive requirement as n_i is the order of the transfer function involving y_i in both the contracted and expanded plant representations.

The General Control Scheme

From the previous section we know that if a stabilizing controller is designed for the expanded system (2.2) and applied to the plant (2.1), then (2.1) will be stabilized, and the closed-loop (2.1) will have the same input/output characteristics as the closed-loop (2.2). This is the basis for the decentralized adaptive control scheme presented here. An indirect adaptive controller is applied at each control station. The identifier at control station i

identifies the ith expanded subsystem with the interconnection terms included; that is, identifier i identifies a model for

$$x_i(t+1) = A_i x_i(t) + b_{ii} u_i(t) + \sum_{j=1, j\neq i}^{N} b_{ij} u_j(t) \tag{2.4}$$

$$y_i(t) = c_i^T x_i(t)$$

which is taken from (2.2b). Equation (2.4) is termed the **ith expanded subsystem** because this is the transfer function that involves $y_i(t)$. A decentralized LQ control law is designed by ignoring the interconnection terms of (2.4); that is, the control law is designed for the local expanded plant

$$x_i(t+1) = A_i x_i(t) + b_{ii} u_i(t) \tag{2.5}$$

$$y_i(t) = c_i^T x_i(t)$$

which is termed the **ith local expanded subsystem** because this is the transfer function from $u_i(t)$ to $y_i(t)$ with the interconnection terms (the b_{ij}'s) ignored (i.e., it is the ith local transfer function). The ith control law is a state feedback type that is designed to use $x_i(t)$ for feedback. In general, $x_i(t)$ is not measurable; therefore, a linear observer is used to estimate these local expanded states. The observer at each control station incorporates controlled inputs from other stations in order to reduce the detrimental effect of ignoring the interconnection

terms when designing the LQ control law for (2.5). As shown in the next section, this significantly improves the overall global stability of the system.

Ignoring the interconnection terms during the design of the LQ control law is a standard decentralized technique. This allows the controllers not to be interdependent on one another. Therefore, if one controller fails, other controllers will still properly perform. The control scheme's success is not solely dependent on any one controller, which makes the scheme very reliable. This is advantageous to the power system problem as it is not uncommon for generators and their controllers to be disconnected from the system.

The rest of this section is broken into four parts with the following subjects addressed: the identifier; the decentralized observer; the decentralized LQ control law; and the integration of the identifier, controller, and observer into an adaptive controller.

Identifier

A recursive multi-input identifier is used at control station i to obtain a model for (2.4). The identifier has the form

$$\hat{\theta}_i(t) = \hat{\theta}_i(t-1) + G_i(t-1)\varepsilon_i(t) \tag{2.6a}$$

$$y_{Mi}(t) = \hat{\theta}_i^T(t-1)\phi_i(t-1) \tag{2.6b}$$

where

$$\varepsilon_i(t) \equiv y_i(t) - y_{Mi}(t) \tag{2.7}$$

$\hat{\theta}_i$ is the parameter estimate vector and ϕ_i is the data vector with

$$\hat{\theta}_i^T(t) = \left[-\hat{a}_{i1}(t), \ldots, -\hat{a}_{in_i}(t), \underset{j=1,\ldots,N}{concat} (\hat{b}_{ij1}(t), \ldots, \hat{b}_{ijn_i}(t)) \right] \tag{2.8a}$$

$$\phi_i^T(t-1) = \left[y_i(t-1), \ldots, y_i(t-n_i), \underset{j=1,\ldots,N}{concat} (u_j(t-1), \ldots, u_j(t-n_i)) \right] \tag{2.8b}$$

where *concat* denotes the appropriate concatenation of the vector entries. This is the usual form for prediction error algorithms (such as projection and recursive-least-squares algorithms), e.g. see [38].

It is assumed the identification algorithm has the following properties:

P1: $|\varepsilon_i(t)| \le \mu_{i1}(t) \| \phi_i(t) \| + \mu_{i2}(t)$ where $\lim_{t \to \infty} \mu_{i1}(t) = \lim_{t \to \infty} \mu_{i2}(t) = 0$, μ_{i1} and μ_{i2} are bounded for all t.

P2: $\| \hat{\theta}_i(t) \|$ is bounded for all t.

P3: $\lim_{t \to \infty} \| \hat{\theta}_i(t) - \hat{\theta}_i(t-1) \| = 0$

These properties hold for many identification algorithms as shown in [38]. The identified model of (2.4) at time t is

$$x_{Mi}(t+1) = \hat{A}_i(t) x_{Mi}(t) + \hat{b}_{ii}(t) u_i(t) + \sum_{j=1, j \neq i}^{N} \hat{b}_{ij}(t) u_j(t) \tag{2.9a}$$

$$y_{Mi}(t) = \hat{c}_i^T x_{Mi}(t)$$

where $x_{Mi} \in \Re^{n_i x n_i}$ and

$$\hat{A}_i(t) \equiv \begin{bmatrix} -\hat{a}_{i1}(t) & 1 & 0 & \dots & 0 \\ -\hat{a}_{i2}(t) & 0 & 1 & \dots & 0 \\ \cdot & \cdot & \cdot & & \cdot \\ \cdot & \cdot & \cdot & & \cdot \\ \cdot & \cdot & \cdot & & \cdot \\ -\hat{a}_{in_i-1}(t) & 0 & 0 & \dots & 1 \\ -\hat{a}_{in_i}(t) & 0 & 0 & \dots & 0 \end{bmatrix}; \quad \hat{b}_{ij}(t) \equiv \begin{bmatrix} \hat{b}_{ij1}(t) \\ \hat{b}_{ij2}(t) \\ \cdot \\ \cdot \\ \cdot \\ \hat{b}_{ijn_i-1}(t) \\ \hat{b}_{ijn_i}(t) \end{bmatrix}; \quad \hat{c}_i \equiv \begin{bmatrix} 1 \\ 0 \\ \cdot \\ \cdot \\ \cdot \\ 0 \end{bmatrix} \qquad (2.9b)$$

Observer

In order to use state feedback control, estimates of the local model states in (2.9) must be obtained. This is done using an observer. At control-station i $x_{Mi}(t)$ is estimated by $\hat{x}_i(t)$, which is obtained from the observer

$$\hat{x}_i(t+1) = \hat{A}_i(t)\hat{x}_i(t) + \hat{b}_{ii}(t)u_i(t) + \sum_{j=1, j\neq i}^{N} \hat{b}_{ij}(t)u_j(t) + k_{oi}(t)(y_i(t) - \hat{c}_i^T\hat{x}_i(t)) \qquad (2.10)$$

where $k_{oi} \in \Re^{n_i}$, and $\hat{A}_i$, $\hat{b}_{ii}$, $\hat{b}_{ij}$ $\hat{c}_i$ are from the identified model (2.9). The observer gain k_{oi} is designed by placing the poles of $(\hat{A}_i^T(t) - \hat{c}_i k_{oi}^T(t))$ inside the unit circle. Since $(\hat{A}_i(t), \hat{c}_i)$ is in observable canonical form, the pole placement only requires n_i additions. Some adaptive controllers which use observers (e.g. see [30], [31], and [35]) force the observers to be deadbeat, but this is overly restrictive. One can use the extra freedom of arbitrarily placing observer poles as an advantage. For example, the observer can be used to obtain a filtering action on measured variables or to lower the magnitude of the controlled input. This is demonstrated in an example later in this chapter.

A general rule for placing observer poles is that they should be closer to the origin of the unit circle than the closed-loop system poles.

The inclusion of the interconnection terms (i.e., the $\hat{b}_{ij}$'s) in (2.10) is unique compared to other decentralized indirect adaptive control schemes, such as those in [30] and [31]. As will be shown in the Global Stability section that follows, inclusion of these terms increases the stability margin of the overall system.

Control Law

The control law at control station i is designed for the local expanded subsystem (2.5). The law is

$$u_i(t) = -k_i^T(t)\hat{x}_i(t) + \alpha_i(t)u_i(t-1) \tag{2.11}$$

where

$$k_i^T(t) = \frac{\tilde{b}_{ii}^T(t)R_i(t)\begin{bmatrix} I^{n_i} \\ 0 \end{bmatrix}\hat{A}_i(t)}{\gamma_i(\omega_{i1} + \omega_{i2} + \tilde{b}_{ii}^T(t)R_i(t)\tilde{b}_{ii}(t))} \tag{2.12a}$$

$$\alpha_i(t) = \frac{\omega_{i2}}{\omega_{i1} + \omega_{i2} + \tilde{b}_{ii}^T(t)R_i(t)\tilde{b}_{ii}(t)} \tag{2.12b}$$

$$R_i(t+1) = Q_i + \tilde{A}_i^T(t)R_i(t)\tilde{A}_i(t) - \frac{\tilde{A}_i^T(t)R_i(t)\tilde{b}_{ii}(t)\tilde{b}_{ii}^T(t)R_i(t)\tilde{A}_i(t)}{\omega_{i1} + \omega_{i2} + \tilde{b}_{ii}^T(t)R_i(t)\tilde{b}_{ii}(t)} \tag{2.12c}$$

with $R_i(0) > 0$ (i.e., $R_i(0)$ is positive definite),

$$\tilde{A}_i(t) \equiv \begin{bmatrix} \frac{1}{\gamma_i}\hat{A}_i(t) & \frac{\omega_{i2}}{\gamma_i^2(\omega_{i1}+\omega_{i2})}\hat{b}_{ii}(t) \\ 0 & \frac{\omega_{i2}}{\gamma_i(\omega_{i1}+\omega_{i2})} \end{bmatrix}, \quad \tilde{b}_{ii}(t) \equiv \begin{bmatrix} \frac{1}{\gamma_i}\hat{b}_{ii}(t) \\ 1 \end{bmatrix}$$

$$Q_i \equiv \begin{bmatrix} \hat{c}_i\hat{c}_i^T & 0 \\ 0 & \frac{\omega_{i1}\omega_{i2}}{\gamma_i^2(\omega_{i1}+\omega_{i2})} \end{bmatrix} \tag{2.13}$$

and R_i, Q_i, $\tilde{A}_i \in \Re^{(n_i+1)x(n_i+1)}$, $\tilde{b}_{ii} \in \Re^{n_i+1}$, $\omega_{i1} \geq 0$, $\omega_{i2} \geq 0$, $\omega_{i1}+\omega_{i2}>0$, $0<\gamma_i \leq 1$. $R_i(t)$ is positive definite and must be maintained symmetric for all t.

An interpretation of the control law is that in the nonadaptive case the steady-state solution to (2.12) minimizes the cost function

$$J_i = \sum_{t=0}^{\infty} \{\gamma_i^{-2t}[x_i^T(t)\hat{c}_i\hat{c}_i^T x_i(t) + \omega_{i1}u_i^2(t) + \omega_{i2}(u_i(t)-u_i(t-1))^2]\} \tag{2.14}$$

for the local subsystem (2.5). This interpretation is obtained by noting (2.12c) is the forward Riccati LQ equation for the cost (2.14), and (2.12a,b) are the LQ gain equations (this is shown in the proof of Lemma 2.1 in the next section). The weight ω_{i1} places a penalty on the magnitude of u_i; the smaller ω_{i1} the more damping expected at the expense of a larger u_i. Weight ω_{i2} penalizes changes in u_i which allows one to temper the rate at which u_i changes. This has been incorporated by others, e.g. see [39]. γ_i is an exponential scaling factor that forces the steady-state closed-loop eigenvalues to be inside a circle of radius γ_i.

Anderson and Moore [5] show this for the standard LQ problem formulation. The smaller γ_i the more damping the controller will add to the system at the expense of larger variations in u_i. Choosing $\gamma_i<1$ is important when controlling an oscillatory system (such as a power system). This is discussed and demonstrated in an example later in this chapter.

Adaptive Controllers

An identifier, observer, and control law are incorporated at each control station to form an indirect adaptive controller. At each time step the following takes place: $y_i(t)$ is sampled and the identifier (2.6) is iterated; the observer gain vector $k_{oi}(t)$ is calculated, and the observer (2.10) is updated; Riccati and gain equations (2.12a,b,c) are updated; and the input equation (2.11) is solved for $u_i(t)$, and $u_i(t)$ is applied to the plant.

Global Stability

In this section conditions of guaranteed overall system stability for the proposed general adaptive controller applied to the plant (2.1) are given. As with most decentralized control strategies, global stability is dependent on the stability of the subsystems and the strength of the interconnections. Lemma 2.1 establishes the stabilizing properties of LQ control law (2.12). The stabilizing of the local expanded subsystem (2.5) using an adaptive con-

troller is established in Lemma 2.2. Global stability conditions for the overall closed-loop system with the proposed decentralized adaptive controller are given in Theorem 2.1. Corollary 2.1 establishes the global stability conditions for the case when communicated controlled inputs are not included in the decentralized observers.

Lemma 2.1

Consider the following general time-varying system:

$$x_i(t+1) = \hat{A}_i(t)x_i(t) + \hat{b}_{ii}(t)u_i(t) \tag{2.15}$$

$$y_i(t) = \hat{c}_i^T x_i(t)$$

If $(\hat{A}_i(t)/\gamma_i, \hat{b}_{ii}(t), \hat{c}_i)$ is uniformly stabilizable and detectable, and both $\|\hat{b}_{ii}(t) - \hat{b}_{ii}(t-1)\|$ and $\|\hat{A}_i(t) - \hat{A}_i(t-1)\| \to 0$, then the control law

$$u_i(t) = -k_i^T x_i(t) + \alpha_i(t)u_i(t-1) \tag{2.16}$$

exponentially stabilizes (2.15), where k_i and α_i are given by (2.12a) and (2.12b), respectively. Also, the closed-loop system is described by

$$\begin{bmatrix} x_i(t+1) \\ v_i(t+1) \end{bmatrix} = \begin{bmatrix} (\hat{A}_i(t) - \hat{b}_{ii}(t)k_i^T(t)) & \alpha_i(t)\hat{b}_{ii}(t) \\ -k_i^T(t) & \alpha_i(t) \end{bmatrix} \begin{bmatrix} x_i(t) \\ v_i(t) \end{bmatrix} \tag{2.17}$$

where $v_i(t+1) \equiv u_i(t)$.

Proof of Lemma 2.1

Define

$$v_i(t+1) \equiv u_i(t) \tag{2.18}$$

$$\hat{u}(t) \equiv \gamma_i^{-t} u_i(t) \tag{2.19}$$

$$z_1(t) \equiv \gamma_i^{-t} x_i(t) \tag{2.20}$$

$$z_2(t+1) \equiv \hat{u}(t) \tag{2.21}$$

$$\hat{y}(t) \equiv \gamma_i^{-t} y_i(t) = \hat{c}_i^T z_1(t) \tag{2.22}$$

where $x_i(t)$, $y_i(t)$, and $u_i(t)$ are those in (2.15). Then (2.15) can be written as

$$z_1(t+1) = \frac{1}{\gamma_i}\hat{A}_i(t) z_1(t) + \frac{1}{\gamma_i}\hat{b}_{ii}(t)\hat{u}(t) \tag{2.23}$$

and (2.14) can be written as

$$J_i = \sum_{t=0}^{\infty}\left\{\hat{y}^2(t) + \frac{\omega_{i2}}{\gamma_i^2} z_2^2(t) + 2[z_1^T(t) \quad z_2(t)]\begin{bmatrix} 0 \\ -\frac{\omega_{i2}}{\gamma_i} \end{bmatrix}\hat{u}(t) + (\omega_{i1} + \omega_{i2})\hat{u}^2(t)\right\} \tag{2.24}$$

Define

$$\tilde{u}(t) \equiv \frac{1}{\omega_{i1} + \omega_{i2}}\begin{bmatrix} 0 & -\omega_{i2} \\ & \gamma_i \end{bmatrix}\begin{bmatrix} z_1(t) \\ z_2(t) \end{bmatrix} + \hat{u}(t) \tag{2.25}$$

Using the results in [40] for performance indices with cross-product terms, (2.24) can be written as

$$J_i = \sum_{t=0}^{\infty}\left\{\hat{y}^2(t) + \frac{\omega_{i1}\omega_{i2}}{\gamma_i^2(\omega_{i1} + \omega_{i2})} z_2^2(t) + (\omega_{i1} + \omega_{i2})\tilde{u}^2(t)\right\} \tag{2.26}$$

Equations (2.21), (2.23), and (2.25) are written as one augmented system

$$\begin{bmatrix} z_1(t+1) \\ z_2(t+1) \end{bmatrix} = \tilde{A}_i(t) \begin{bmatrix} z_1(t) \\ z_2(t) \end{bmatrix} + \tilde{b}_{ii}(t)\tilde{u}(t) \tag{2.27}$$

where $\tilde{A}_i$ and $\tilde{b}_{ii}$ are from (2.13).

If the system consisting of (2.27) and cost function (2.26) is uniformly stabilizable and detectable, then one update per iteration of the Riccati equation corresponding to (2.26) and application of the corresponding feedback gains guarantees that the closed-loop system is stabilized (this is shown in [35]). Applying this result while using (2.18)-(2.22) and (2.25) results in the feedback function (2.16) with (2.12a,b,c) providing guaranteed stability to (2.15) if $(\hat{A}_i/\gamma_i,\ \hat{b}_{ii},\ \hat{c}_i)$ is uniformly stabilizable and detectable. The closed-loop system (2.17) is obtained by directly applying (2.16) to (2.15).

Q.E.D.

Lemma 2.2

Consider the local expanded subsystem (2.5) with an indirect adaptive controller consisting of an identifier, an observer and a control law. The identifier is assumed to have properties (P1)-(P3), given above (2.9), where

$$\phi_i^T(t-1) = [y_i(t-1) \quad \dots \quad y_i(t-n_i) \quad u_i(t-1) \quad \dots \quad u_i(t-n_i)] \tag{2.28}$$

and identifies the local plant model

$$x_{Mi}(t+1) = \hat{A}_i(t)x_{Mi}(t) + \hat{b}_{ii}(t)u_i(t) \tag{2.29}$$

$$y_{Mi}(t) = \hat{c}_i^T x_{Mi}(t)$$

The observer is

$$\hat{x}_i(t+1) = \hat{A}_i(t)\hat{x}_i(t) + \hat{b}_{ii}(t)u_i(t) + k_{oi}(t)\,(y_i(t) - \hat{c}_i^T\hat{x}_i(t)) \tag{2.30}$$

and the control law is given by (2.11) and (2.12). The resultant closed-loop system is stable if

(i) $(\hat{A}_i(t)/\gamma_i,\ \hat{b}_{ii}(t),\ \hat{c}_i)$ is observable for all t and uniformly stabilizable,

(ii) $k_{oi}(t)$ is chosen to place the eigenvalues of $(\hat{A}_i^T(t) - \hat{c}_i k_{oi}^T(t))$ inside the unit circle at each time t.

Also, the closed-loop system is described by

$$z_i(t+1) = A_{ci}(t)z_i(t) + Y_i(t) \tag{2.31}$$

where

$$z_i^T(t) \equiv [\phi_i^T(t-1) \quad x_{Mi}^T(t) \quad v_i(t) \quad e_i^T(t)] \tag{2.32}$$

$$v_i(t+1) \equiv u_i(t) \tag{2.33}$$

$$e_i(t) \equiv x_{Mi}(t) - \hat{x}_i(t) \tag{2.34}$$

$$A_{ci}(t) \equiv \begin{bmatrix} F & D_{i1}(t) & D_{i2}(t) & D_{i3}(t) \\ 0 & (\hat{A}_i(t) - \hat{b}_{ii}(t)k_i^T(t)) & \alpha_i(t)\hat{b}_{ii}(t) & \hat{b}_{ii}(t)k_i^T(t) \\ 0 & -k_i^T(t) & \alpha_i(t) & k_i^T(t) \\ 0 & 0 & 0 & (\hat{A}_i(t) - k_{oi}(t)\hat{c}_i^T) \end{bmatrix} \tag{2.35a}$$

$$F \equiv I^2 \otimes B\ ; \quad B \equiv \begin{bmatrix} 0 & 0 \\ I^{n_i-1} & 0 \end{bmatrix} \tag{2.35b}$$

$$D_{i1}(t) \equiv \begin{bmatrix} \hat{c}_i^T \\ 0 \\ \cdot \\ \cdot \\ \cdot \\ 0 \\ -k_i^T(t) \\ 0 \\ \cdot \\ \cdot \\ \cdot \\ 0 \end{bmatrix}; \quad D_{i2}(t) \equiv \begin{bmatrix} 0 \\ 0 \\ \cdot \\ \cdot \\ \cdot \\ 0 \\ \alpha_i(t) \\ 0 \\ \cdot \\ \cdot \\ \cdot \\ 0 \end{bmatrix}; \quad D_{i3}(t) \equiv \begin{bmatrix} 0 \\ 0 \\ \cdot \\ \cdot \\ \cdot \\ 0 \\ k_i^T(t) \\ 0 \\ \cdot \\ \cdot \\ \cdot \\ 0 \end{bmatrix} \qquad (2.35c)$$

$$Y_i^T(t) \equiv [V_i^T(t) \quad 0 \quad 0 \quad -\varepsilon_i(t)k_{oi}^T(t)] \qquad (2.36a)$$

$$V_i^T(t) \equiv [\varepsilon_i(t) \quad 0 \quad \ldots \quad 0] \qquad (2.36b)$$

with $F \in \Re^{2n_i x 2n_i}$, $B \in \Re^{n_i x n_i}$, D_{i1} and $D_{i3} \in \Re^{2n_i x n_i}$, $D_{i2} \in \Re^{2n_i}$, $Y_i \in \Re^{4n_i+1}$, $V_i \in \Re^{2n_i}$.

Proof of Lemma 2.2

Using (2.7), the observer (2.30) is written as

$$\hat{x}_i(t+1) = \hat{A}_i(t)\hat{x}_i(t) + \hat{b}_{ii}(t)u_i(t) + k_{oi}(t)(y_{Mi}(t) - \hat{c}_i^T\hat{x}_i(t)) + k_{oi}(t)\varepsilon_i(t) \qquad (2.37)$$

where y_{Mi} is from (2.29). Equations (2.37) and (2.29) are combined using (2.34) as

$$e_i(t+1) = (\hat{A}_i(t) - k_{oi}(t)\hat{c}_i^T)e_i(t) - k_{oi}(t)\varepsilon_i(t) \qquad (2.38)$$

Control law (2.11) is rewritten using (2.33) and (2.34) as

$$u_i(t) = -k_i^T(t)x_{Mi}(t) + k_i^T(t)e_i(t) + \alpha_i(t)v_i(t) \qquad (2.39)$$

Control (2.39) is applied to the local plant model (2.29) resulting in

$$x_{Mi}(t+1) = (\hat{A}_i(t) - \hat{b}_{ii}(t)k_i^T(t))x_{Mi}(t) + \hat{b}_{ii}(t)k_i^T(t)e_i(t) + \hat{b}_{ii}(t)\alpha_i(t)v_i(t) \qquad (2.40)$$

Using (2.7), (2.28), and (2.39) it is easy to show that the local subsystem can be written as

$$\phi_i(t) = F\phi_i(t-1) + [D_{i1}(t) \quad D_{i2}(t) \quad D_{i3}(t)]\begin{bmatrix} x_{Mi}(t) \\ v_i(t) \\ e_i(t) \end{bmatrix} + V_i(t) \qquad (2.41)$$

where F, D_{i1}, D_{i2}, D_{i3}, and V_i are from (2.35b,c) and (2.36b). The closed-loop system is represented by combining (2.33) and (2.38)-(2.41) to form (2.31). With $(\hat{A}_i(t), \hat{c}_i)$ given to be observable, bounded $k_{oi}(t)$ are readily available to place eigenvalues of $(\hat{A}_i^T(t) - \hat{c}_i k_{oi}^T(t))$ inside the unit circle for all t. Because of identifier properties (P2) and (P3), $(\hat{A}_i^T(t) - \hat{c}_i k_{oi}^T(t))$ will boundly converge to a stable matrix, which implies stability of $(\hat{A}_i^T(t) - \hat{c}_i k_{oi}^T(t))$. Again from (P2) and (P3), stability of $(\hat{A}_i^T(t) - \hat{c}_i k_{oi}^T(t))$ implies stability of $(\hat{A}_i(t) - k_{oi}\hat{c}_i^T(t))$ (see [35]). Using this assumption and Lemma 2.1, it is easy to see that $A_{ci}(t)$ is a stable matrix because the block diagonal terms are stable. If identifier properties (P1)-(P3) are satisfied and $(\hat{A}_i/\gamma_i, \hat{b}_{ii}, \hat{c}_i)$ is uniformly stabilizable, then proof 9.1 in [35] can be used to show stability of (2.31).

Q.E.D.

Theorem 2.1

Consider the multi-control-station plant (2.1) with adaptive controllers applied at each station. Each adap-

tive controller consists of an identifier having properties (P1)-(P3), observer (2.10), and control law (2.11) and (2.12). The closed-loop system is stable if

(i) There exists $(P_1, \ldots, P_N) \in \Re^{(4n_i+1)x(4n_i+1)}$ with $P_i>0$ and positive functions $(\sigma_1(t), \ldots, \sigma_N(t))$ such that

$$(v^T A_{ci}^T(t) + Y_i^T(t))P_i(A_{ci}(t)v + Y_i(t)) - v^T P_i v \le -\sigma_i(t)\|v\| \quad (2.42)$$

for $i=1,2,\ldots,N$. A_{ci} and Y_i are from (2.35) and (2.36), and $v \in \Re^{4n_i+1}$ is an arbitrary nonzero vector.

(ii) There exists positive scalars $(\beta_1, \ldots, \beta_N)$ such that

$$|v^T P_i v - w^T P_i w| \le \beta_i \|v - w\| \; ; \quad i = 1,2,\ldots,N \quad (2.43)$$

where v and $w \in \Re^{4n_i+1}$ are arbitrary nonzero vectors.

(iii) $$(\alpha_i^2(t) + 2\|k_i(t)\|^2)^{1/2} \sum_{j=1, j\neq i}^{N} \beta_j \|\hat{b}_{ji}(t)\| < \sigma_i(t) \; ; \quad i = 1,2,\ldots,N \quad (2.44)$$

Proof of Theorem 2.1

In this proof Euclidean norm properties (NP1)-(NP4) are used. Let $A \in \Re^{nxn}$ be an arbitrary matrix, and let x and $y \in \Re^n$ be arbitrary vectors. The properties are

NP1: $\|x+y\| \le \|x\| + \|y\|$

NP2: $\|Ax\| \le \|A\| \, \|x\|$

NP3: $\|A\|^2 = trace(A^T A)$

NP4: $\|x\|^2 = trace(xx^T)$

The identifier at station i identifies a model for the expanded subsystem (2.4) which is given by (2.9). Define

$$e_i(t) \equiv x_{Mi}(t) - \hat{x}_i(t); \quad i = 1,2,\ldots,N \tag{2.45}$$

$$v_i(t+1) \equiv u_i(t); \quad i = 1,2,\ldots,N \tag{2.46}$$

where x_{Mi} is from (2.9a) and $\hat{x}_i$ is from the observer (2.10). Using (2.7) it is easy to show that

$$e_i(t+1) = (\hat{A}_i(t) - k_{oi}(t)\hat{c}_i^T)e_i(t) - k_{oi}(t)\varepsilon_i(t); \quad i = 1,2,\ldots,N \tag{2.47}$$

Control law (2.11) can be written using (2.45) and (2.46) as

$$u_i(t) = -k_i^T(t)x_{Mi}(t) + k_i^T(t)e_i(t) + \alpha_i(t)v_i(t); \quad i = 1,2,\ldots,N \tag{2.48}$$

and (2.9a) is

$$\begin{aligned} x_{Mi}(t+1) = &(\hat{A}_i(t) - \hat{b}_{ii}(t)k_i^T(t))x_{Mi}(t) + \hat{b}_{ii}(t)k_i^T(t)e_i(t) + \alpha_i(t)\hat{b}_{ii}(t)v_i(t) \\ &+ \sum_{j=1, j\neq i}^{N} \hat{b}_{ij}(t)(-k_j^T(t)x_{Mj}(t) + k_j^T(t)e_j(t) + \alpha_j(t)v_j(t)); \quad i = 1,2,\ldots,N \end{aligned} \tag{2.49}$$

Using (2.7) and (2.48) the input/output relation at the ith expanded subsystem is

$$\tilde{\phi}_i(t) = F\tilde{\phi}_i(t-1) + [D_{i1}(t) \quad D_{i2}(t) \quad D_{i3}(t)]\begin{bmatrix} x_{Mi}(t) \\ v_i(t) \\ e_i(t) \end{bmatrix} + V_i(t); \quad i = 1,2,\ldots,N \tag{2.50}$$

where F, D_{i1}, D_{i2}, D_{i3}, and V_i are from (2.35b,c) and (2.36b), and

$$\tilde{\phi}_i^T(t-1) = [y_i(t-1) \quad \ldots \quad y_i(t-n_i) \quad u_i(t-1) \quad \ldots \quad u_i(t-n_i)]; \quad i = 1,2,\ldots,N \tag{2.51}$$

The closed-loop system is described by combining (2.46) through (2.50) as

$$z_i(t+1) = A_{ci}(t)z_i(t) + Y_i(t) + \sum_{j=1, j\neq i}^{N} A_{cij}(t)z_j(t); \quad i = 1,2,\ldots,N \tag{2.52}$$

where A_{ci} and Y_i are defined in Lemma 2.2, $z_i(t) \equiv [\tilde{\phi}_i^T(t-1)\ x_{Mi}^T(t)\ v_i(t)\ e_i^T(t)]$, and

$$A_{cij}(t) \equiv \begin{bmatrix} 0 & 0 & 0 & 0 \\ 0 & -\hat{b}_{ij}(t)k_j^T(t) & \alpha_j(t)\hat{b}_{ij}(t) & \hat{b}_{ij}(t)k_j^T(t) \\ 0 & 0 & 0 & 0 \\ 0 & 0 & 0 & 0 \end{bmatrix} \tag{2.53}$$

with $A_{cij} \in \Re^{(4n_i+1)x(4n_i+1)}$. To investigate the stability of (2.52) we form the positive-definite Liapunov candidate function

$$L(t) = \sum_{i=1}^{N} z_i^T(t)P_i z_i(t) \tag{2.54}$$

where each $P_i>0$ and of appropriate dimension. Now

$$\Delta L(t) \equiv L(t+1) - L(t) \tag{2.55}$$

$$\begin{aligned} &= \sum_{i=1}^{N} \{[\left(z_i^T(t)A_{ci}^T + Y_i^T + \sum_{j=1, j\neq i}^{N} z_j^T(t)A_{cij}^T\right)P_i\left(A_{ci}z_i(t) + Y_i + \sum_{j=1, j\neq i}^{N} A_{cij}z_j(t)\right) \\ &\quad -(z_i^T(t)A_{ci}^T + Y_i^T)P_i(A_{ci}z_i(t) + Y_i)] \\ &\quad +[(z_i^T(t)A_{ci}^T + Y_i^T)P_i(A_{ci}z_i(t) + Y_i) - z_i^T(t)P_i z_i(t)]\} \end{aligned} \tag{2.56}$$

where the dependence on t has been dropped in (2.56) for simplicity of writing the equation. Assume conditions (i) and (ii) are satisfied in the theorem; then

$$\Delta L(t) \leq \sum_{i=1}^{N}\left\{\beta_i \left\| \sum_{j=1, j\neq i}^{N} A_{cij}(t)z_j(t) \right\| - \sigma_i(t)\|z_i(t)\|\right\} \tag{2.57}$$

$$\leq \sum_{i=1}^{N}\left\{-\sigma_i(t)\|z_i(t)\| + \beta_i \sum_{j=1, j\neq i}^{N}\|A_{cij}(t)\|\,\|z_j(t)\|\right\} \tag{2.58}$$

$$= \sum_{i=1}^{N}\left\{\left(-\sigma_i(t) + \sum_{j=1, j\neq i}^{N}\beta_j\|A_{cji}(t)\|\right)\|z_i(t)\|\right\} \tag{2.59}$$

Equation (2.59) is guaranteed to be negative definite if

$$\sum_{j=1, j\neq i}^{N}\beta_j\|A_{cji}(t)\| < \sigma_i(t); \quad i = 1,2,\ldots,N \tag{2.60}$$

Using norm properties (NP3), (NP4), and the fact that A_{cji} is taken from (2.53), (2.44) directly follows from (2.60). Because (2.2) is an expansion of (2.1), stabilization of (2.2) implies stabilization of (2.1); therefore, any conditions for stabilization of (2.2) also apply to (2.1). This last point is discussed in detail in the first section of this chapter.

Q.E.D.

Corollary 2.1

Consider the multi-control-station plant described by (2.1). Adaptive indirect controllers are again applied to each control station. Each adaptive controller consists of an identifier having properties (P1)-(P3), an observer, and control law (2.11) and (2.12). The observer at station i in this case is

$$\hat{x}_i(t+1) = \hat{A}_i(t)\hat{x}_i(t) + \hat{b}_{ii}(t)u_i(t) + k_{oi}(t)\left(y_i(t) - c_i^T\hat{x}_i(t)\right) \tag{2.61}$$

The overall closed-loop system is stable if the following are satisfied:

(i) Condition (i) of Theorem 2.1 is satisfied.

(ii) Condition (ii) of Theorem 2.1 is satisfied.

(iii) $$\sqrt{2}(\alpha_i^2(t)+2\|k_i(t)\|^2)^{1/2}\sum_{j=1,j\neq i}^{N}\beta_j\|\hat{b}_{ji}(t)\|<\sigma_i(t);\quad i=1,2,\ldots,N \qquad (2.62)$$

Proof of Corollary 2.1

The proof follows the same lines as that of Theorem 2.1 except the observer of (2.61) is used at each control station.

Q.E.D.

Remarks on Theorem 2.1 and Corollary 2.1

Condition (i) of Theorem 2.1 and Corollary 2.1 can only be satisfied if the local stability condition of Lemma 2.2 is satisfied. If the local stability condition is satisfied, then in most cases condition (i) can be satisfied. Also, in most cases condition (ii) can be satisfied. This leave (iii) as the most important condition.

Condition (iii) of Theorem 2.1 and Corollary 2.1 give global stability conditions in terms of the expanded system interconnection terms estimated by the identifiers (the $\hat{b}_{ij}$'s). As is typical of most decentralized control problems, the weaker the subsystem interconnections the more likely the system will be globally stable (this is easily seen from condition (iii)). It appears from condition (iii) that the smaller the feedback gains k_i and α_i, the more likely condition (iii) will be satisfied. But, this

may not be true because the β_i's and σ_i's are dependent on the local stability of the subsystems with interconnections ignored.

The observer (2.61) in Corollary 2.1 differs from that in (2.10) only by the exclusion of the $\hat{b}_{ij}$ terms. By comparing condition (iii) of Theorem 2.1 and Corollary 2.1, one can see that global stability is more likely if the $\hat{b}_{ij}$'s are included in the decentralized observers (by a factor of $\sqrt{2}$). The $\sqrt{2}$ factor in Corollary 2.1 implies that the Liapunov function will decrease faster for the case where communicated information is included in the observer (i.e., the use of observer (2.10)). This in turn implies that better damping can result from using the communicated information in the observers for the power system problem.

The Specific Control Scheme to be Implemented

In the second section of this chapter, a general decentralized adaptive control strategy was presented. The general presentation of the controller left many options for choosing a specific identification scheme. In this section a specific identification algorithm is proposed. Also, modifications are made to the observer and control law in order to make the adaptive controller more robust and more easily implemented.

The purpose of the identifier is to identify a parameter vector $\hat{\theta}_i(t)$ in (2.6b) such that properties (P1)-(P3) are

satisfied. Many recursive identifications algorithms are contained in the literature that satisfy these properties under weak assumptions (such as persistent excitation). Two well known algorithms are the projection and least-squares algorithms [38], with recursive-least-squares (RLS) being the most popular [41]. RLS is popular because it has good convergence properties in the presence of Gaussian measurement noise; it is the method used for the adaptive controllers applied in this thesis. The RLS method is derived by minimizing a cost function that is the sum of squared errors over time, where the errors are the difference between the actual system output and the identifier output.

The standard RLS equations applied to the expanded subsystem (2.4) are given in [38] and are

$$\hat{\theta}_i(t) = \hat{\theta}_i(t-1) + \frac{P_i(t-1)\phi_i(t-1)\varepsilon_i(t)}{\lambda_i + \phi_i^T(t-1)P_i(t-1)\phi_i(t-1)} \tag{2.63a}$$

$$P_i(t) = \frac{1}{\lambda_i}\left[P_i(t-1) - \frac{P_i(t-1)\phi_i(t-1)\phi_i^T(t-1)P_i(t-1)}{\lambda_i + \phi_i^T(t-1)P_i(t-1)\phi_i(t-1)}\right] \tag{2.63b}$$

which can easily be placed in the form of (2.6b). Vectors $\hat{\theta}_i$ and ϕ_i are defined in (2.8); P_i is termed the covariance matrix; ε_i is defined in (2.7); and λ_i is an exponential forgetting factor [38]. The forgetting factor is used to enhance the time-varying identification properties of the RLS algorithm. Using λ_i is (2.63) is equivalent to weight-

ing past errors in the cost function exponentially. By having $\lambda_i < 1$, past errors are weighted less than more recent ones. Typical values of λ_i are in the 0.97 to 1.0 range.

The RLS identifier FORTRAN subroutine used for system simulations in this thesis is taken from [41] with slight modifications. It is termed the Corrector-Least-Squares (CLS) subroutine. The RLS equations are solved using a UDU^T covariance factorization which enhances the numerical robustness of the algorithm. Many options are available with the CLS subroutine; most of these options are special variations of the standard RLS algorithm and are not used in the simulation results in this thesis. The calling statement for the CLS subroutine along with a description of the variables and of the modifications are contained in Appendix A.

One important option of the CLS subroutine that is used with the simulations in this thesis is the "ratio test." The ratio test is described in detail in [41] and to a lesser extent in [42]. It is a novel richness test used to help prevent the problem of covariance blowup. When the input to a system does not sufficiently excite the system, the RLS algorithm will often blowup at a rate of $1/\lambda_i$ (this is termed covariance blowup). When the ratio test detects this blowup, the CLS subroutine stops iterating the RLS equations until the blowup is no longer detected. The blowup is detected by monitoring the growth of the trace of

the covariance matrix for a given number of time steps.

Not only is covariance blowup a problem when the plant input is not sufficiently rich, improper model identification can also occur. Therefore, it is important to always make an attempt to keep the system excited when the identifier is updating parameters. For the adaptive control simulations conducted in this thesis, the system is kept excited by adding a low-level probing signal to the plant input. For the first seven seconds of all simulations the plant input is a probing signal of ± 0.004 with random switches made every three samples (with the control loop open). After seven seconds the control loop is closed, and the probing signal is reduced to ± 0.001 and is added to the plant input from the adaptive controller.

It is well known that LQ control with a full-order observer has poor robustness properties, e.g. see [5]. To help alleviate this problem, it is suggested in [5] that when possible a reduced-order observer should be used to estimate system states. To incorporate this into the adaptive control scheme used here, the observer of (2.10) is replaced with the following reduced-order one taken from [40]:

$$\hat{x}_i^T(t) \equiv [\hat{x}_{iA}(t) \quad \hat{x}_{iB}^T(t)] \tag{2.64a}$$

$$\hat{x}_{iA}(t) = y_i(t) \tag{2.64b}$$

$$\hat{x}_{iB}(t) = \zeta_i(t) + k_{oi} y_i(t) \tag{2.64c}$$

$$\zeta_i(t+1) = \hat{K}_{oi}\zeta_i(t) + \left(h_i + \hat{a}_{i1}(t)k_{oi} - \begin{bmatrix} \hat{a}_{i2}(t) \\ \hat{a}_{i3}(t) \\ \cdot \\ \cdot \\ \cdot \\ \hat{a}_{in_i}(t) \end{bmatrix} \right) y_i(t) + \left(\begin{bmatrix} \hat{b}_{ii2}(t) \\ \hat{b}_{ii3}(t) \\ \cdot \\ \cdot \\ \cdot \\ \hat{b}_{iin_i}(t) \end{bmatrix} - k_{oi}\hat{b}_{ii1}(t) \right) u_i(t)$$

$$+ \sum_{j=1, j\neq i}^{N} \left(\begin{bmatrix} \hat{b}_{ij2}(t) \\ \hat{b}_{ij3}(t) \\ \cdot \\ \cdot \\ \cdot \\ \hat{b}_{ijn_i}(t) \end{bmatrix} - k_{oi}\hat{b}_{ij1}(t) \right) u_j(t) \qquad (2.64d)$$

where $k_{oi}^T \equiv [k_{oi1} \quad k_{oi2} \quad \dots \quad k_{oin_i}]$,

$$\hat{K}_{oi} \equiv \begin{bmatrix} -k_{oi1} & 1 & 0 & \dots & 0 \\ -k_{oi2} & 0 & 1 & \dots & 0 \\ \cdot & \cdot & \cdot & & \cdot \\ \cdot & \cdot & \cdot & & \cdot \\ \cdot & \cdot & \cdot & & \cdot \\ -k_{oi(n_i-2)} & 0 & 0 & \dots & 1 \\ -k_{oi(n_i-1)} & 0 & 0 & \dots & 0 \end{bmatrix}; \qquad h_i \equiv \hat{K}_{oi}k_{oi} \qquad (2.65)$$

and $\hat{x}_i \in \Re^{n_i}$, $\hat{x}_{iA} \in \Re$, $\hat{K}_{oi} \in \Re^{(n_i-1)x(n_i-1)}$, and $\hat{x}_{iB}$, ζ_i, k_{oi}, $h_i \in \Re^{n_i-1}$.

The elements of the reduced-order observer gain vector k_{oi} are the coefficients of the desired observer characteristic polynomial. The reduced-order observer of (2.64) differs from its full-order counterpart (2.10) by taking advantage of the fact that $y_i(t)$ is one of the states to be estimated. Other control station inputs (the u_j's) are incorporated into (2.64) in a similar way as they were into (2.10). Although the stability properties of the control

scheme given in Theorem 2.1 and Corollary 2.1 were developed using full-order observers, it is very reasonable to expect similar properties when reduced-order observers are used. This is because both types of observers are designed to give state estimates and to be stable.

When a discrete-time adaptive controller is implemented, every attempt should be made to decrease delay times. Delay times occur when calculations must be made to obtain $u_i(t)$ after $y_i(t)$ has been sampled. Using the control law of (2.11) and (2.12) requires (2.63a), (2.12a), and (2.12b) to all be iterated after $y_i(t)$ is sampled and before $u_i(t)$ is applied to the system. In most adaptive control cases, it is expected that the plant is not highly time varying; therefore, very small changes are expected in the control law feedback gains from one sample to the next. Using this reasoning, one would not expect the properties of the adaptive controller to change if control calculation equation (2.11) is replaced with

$$u_i(t) = -k_i^T(t-1)\hat{x}_i(t) + \alpha_i(t-1)u_i(t-1) \tag{2.66}$$

Using (2.66) in place of (2.11) significantly reduces the delay time of the adaptive controller. Now (2.63a), (2.12a), and (2.12b) are allowed a full sample period for evaluation.

Figure 3 shows the adaptive controller at control station i. The controller is implemented using the following steps: 1) output $y_i(t)$ is sampled at time t; 2) equations

(2.64c) and (2.66) are immediately solved to obtain $u_i(t)$, and $u_i(t)$ is applied to the plant; 3) $u_i(t)$ is communicated to other control stations; 4) the RLS identifier in (2.63) is iterated using the sampled $y_i(t)$; 5) observer equation (2.64d) is iterated to obtain $\zeta_i(t+1)$; and 6) the Riccati and gain equations (2.12a,b,c) are iterated to obtain $k_i(t)$ and $\alpha_i(t)$. Step 3 is allowed one full sample period. Step 4 must be completed before 5 and 6 which may be executed simultaneously. Step 2 must be computed as fast as possible; but, since it only involves two vector multiplications of order n_i-1, use of a modern computer makes delay time insignificant for sample periods on the order of 10 milliseconds or greater. Conventional computer computation times for algorithms similar to those described here are discussed in [43].

To perform the adaptive controller simulations in this thesis, the adaptive control algorithms were coded using FORTRAN subroutines. These subroutines are contained in the Appendix A. The subroutine that implements the identifier is taken from [41] and was discussed earlier. A subroutine that iterates the reduced-order observer equation (2.64d) once per call is used. Observer equation (2.64c) and control calculation (2.66) are contained in one subroutine so that $u_i(t)$ can be calculated immediately after $y_i(t)$ is sampled. A fourth subroutine is used to iterate control law equations (2.12a,b,c).

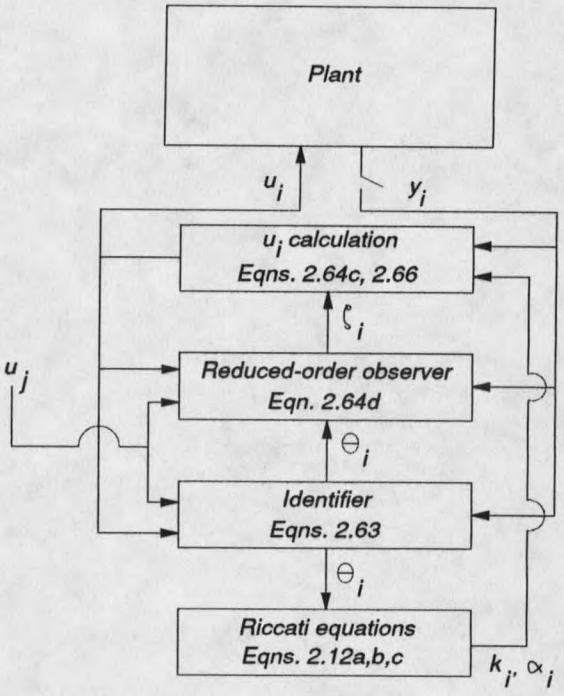

Figure 3. Adaptive controller at control station i.

Properties of the Control Scheme

The decentralized indirect adaptive control scheme has a number of unique properties when compared to similar schemes proposed in the literature (such as [30] and [31]). In this section these properties are demonstrated and discussed using several examples.

Example 1

An advantage of the control scheme is that it guarantees certain stability limits (see Theorem 2.1). If independent adaptive controllers are applied to the plant at each control station with no communication between

controllers, the stability limits become weaker. The stability limits are theoretical analysis results. Do they imply the proposed control scheme will perform much better over the case where independent adaptive controllers are used? Obviously, the answer to this question depends on the plant. This example demonstrates that the proposed scheme can result in much better performance.

Consider the unstable three-oscillator overlapping interconnected plant with 2 control stations:

$$\dot{x}_1 = \begin{bmatrix} 0 & 1 \\ -4\pi^2 & 0 \end{bmatrix} x_1 + \begin{bmatrix} 0 \\ 8 \end{bmatrix} u_1$$

$$\dot{x}_2 = \begin{bmatrix} 0 & 1 \\ -0.64\pi^2 & 0.1 \end{bmatrix} x_2 + \begin{bmatrix} 0 \\ -7 \end{bmatrix} u_1 + \begin{bmatrix} 8 \\ 0 \end{bmatrix} u_2 \qquad (2.67)$$

$$\dot{x}_3 = \begin{bmatrix} 0 & 1 \\ -5\pi^2 & 0 \end{bmatrix} x_3 + \begin{bmatrix} 0 \\ 9 \end{bmatrix} u_2$$

$$y_1 = [5 \quad 0] x_1 + [6 \quad 0] x_2$$

$$y_2 = [7 \quad 0] x_2 + [9 \quad 0] x_3$$

which is in a continuous-time form corresponding to (2.1a) with N=2, m=3, and $\bar{n}_1$=$\bar{n}_2$=$\bar{n}_3$=2. Subsystems 1 and 3 are undamped oscillators that are only connected to control stations 1 and 3 respectively. Subsystem 2 is a slightly negatively damped oscillator that is connected to both control stations. In order to apply the proposed decentralized adaptive controllers, n_1 and n_2 corresponding to the expanded system representation must be known. As stated in

the first section of this chapter, n_i is the order of the transfer function involving y_i. For this system n_1=4 and n_2=4.

Indirect adaptive controllers are applied at each control station, with the objective of adding damping to the system. The discrete-time controllers are implemented by using a 0.1 second sample period. Two different control cases are compared. For the first case, termed the "communication" case, the proposed specific control scheme presented in the third section of this chapter is used. With the second case, termed the "no communication" case, independent adaptive controllers are used at each control station. This is the same as used in the first case, but no communication is used between controllers. To implement the second case, the communication terms (i.e. the terms multiplying the u_j's) in the observer equation (2.64c) are not included, and the communicated terms are also not included in the identifiers. The identifiers, observers, and LQ control laws for both cases have the following settings: LQ control laws -- $\omega_{11}=\omega_{12}=1$, $\omega_{21}=\omega_{22}=2$, $\gamma_1=\gamma_2=0.98$; both local observers are designed to have poles at 0.5 and $0.5e^{\pm j30°}$; identifiers -- $\lambda_1=\lambda_2=0.97$. The absolute magnitudes of u_1 and u_2 are required to be less than 5.

To demonstrate the differences between the two control cases, a delta-function type disturbance hits all state variables in the system at 20 seconds. Figures 4 and 5

show the open-loop response of y_1 and y_2. System variables y_1 and u_1 are shown in Figures 6 and 7 for the two control cases; y_2 and u_2 are shown in Figures 8 and 9. As can be seen from the figures, the proposed control scheme dampens the system while the independent controllers have no stabilizing effect (in fact they have a negative effect on the system).

Under the conditions used in this example, communication between controllers is required for stability. Communicated information is critical to both the identifiers and observers. One expects these results because subsystem interconnections in (2.67) are relatively strong.

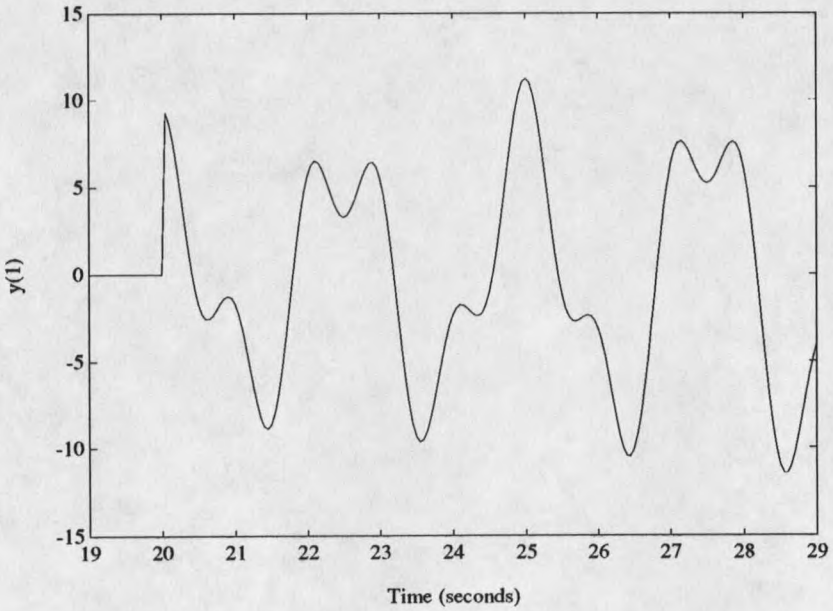

Figure 4. Example 1, open-loop response of y_1.

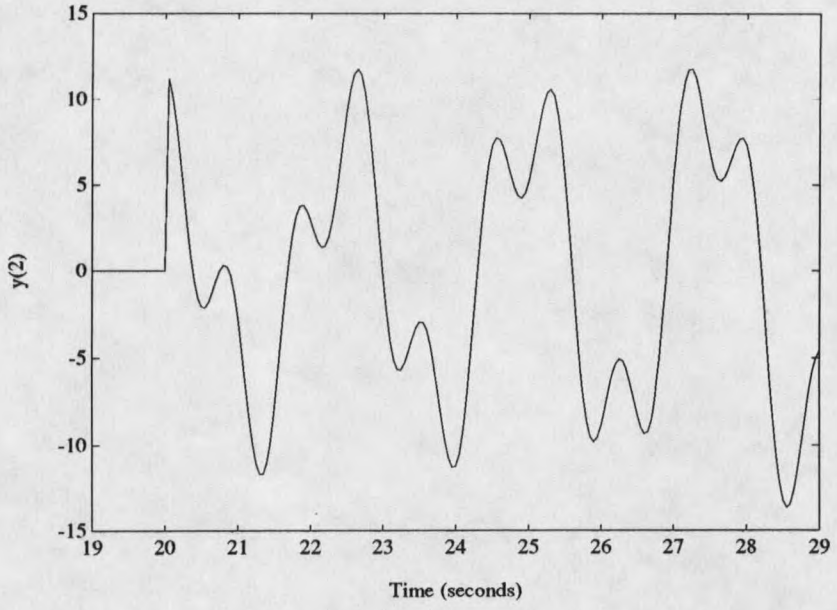

Figure 5. Example 1, open-loop response of y_2.

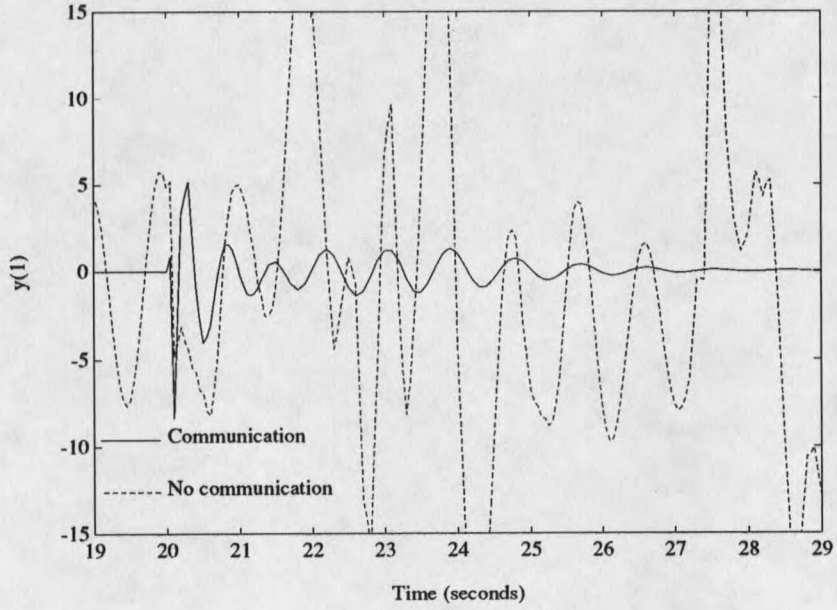

Figure 6. Example 1, closed-loop response of y_1.

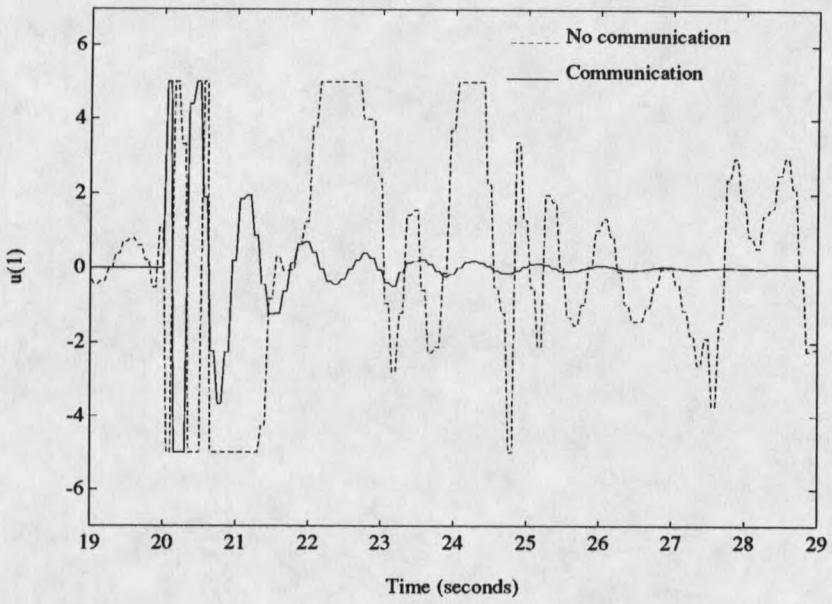

Figure 7. Example 1, closed-loop response of u_1.

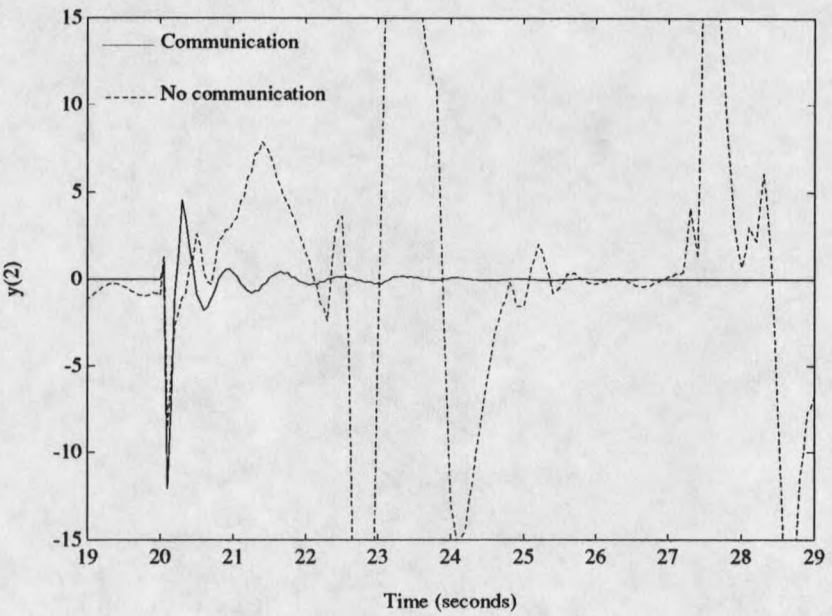

Figure 8. Example 1, closed-loop response of y_2.

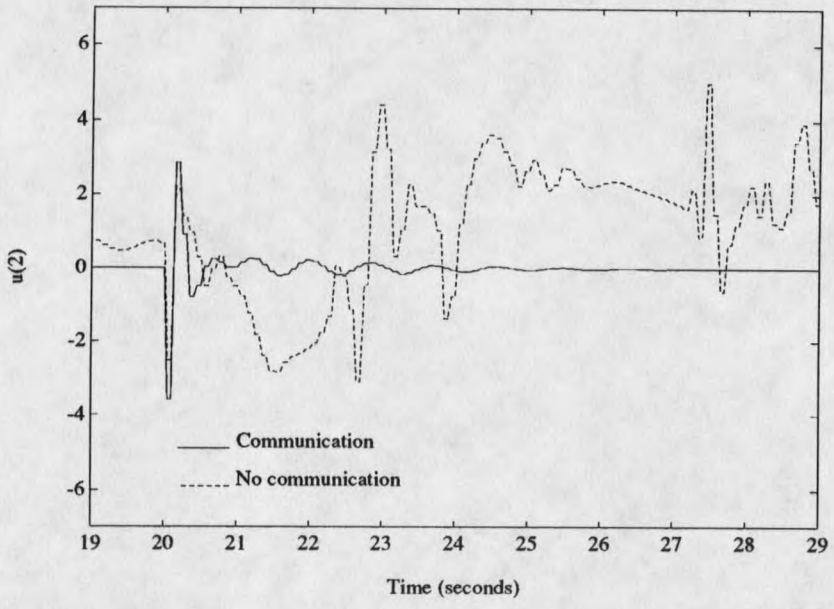

Figure 9. Example 1, closed-loop response of u_2.

Example 2

Other decentralized adaptive control schemes in the literature (such as [30] and [31]) have used communicated information in the identifiers but not in the observers. The use of the communicated information in the observer is unique to the control scheme proposed in this thesis. From Theorem 2.1 and Corollary 2.1 it is seen that the use of communicated inputs in the observer design improve global stability limits. This example further demonstrates this.

Again consider the plant described by (2.67). The decentralized adaptive control scheme is applied to the plant with two cases compared. In one case the communica-

tion terms are included in the observers while in the other these terms are excluded. The same adaptive controller settings as in Example 1 are used here.

The same disturbance as used in Example 1 is applied to the system. Figure 10 shows y_1 for the two control cases, and corresponding u_1's are shown in Figure 11. Figures 12 and 13 show y_2 and u_2.

Note that in the case where communicated information is included in the observer, much better damping results. By studying Theorem 2.1 and Corollary 2.1, one expects this result because the subsystem interconnections in (2.67) are relatively strong. This demontrates the advantage of using communicated information in the decentralized observers.

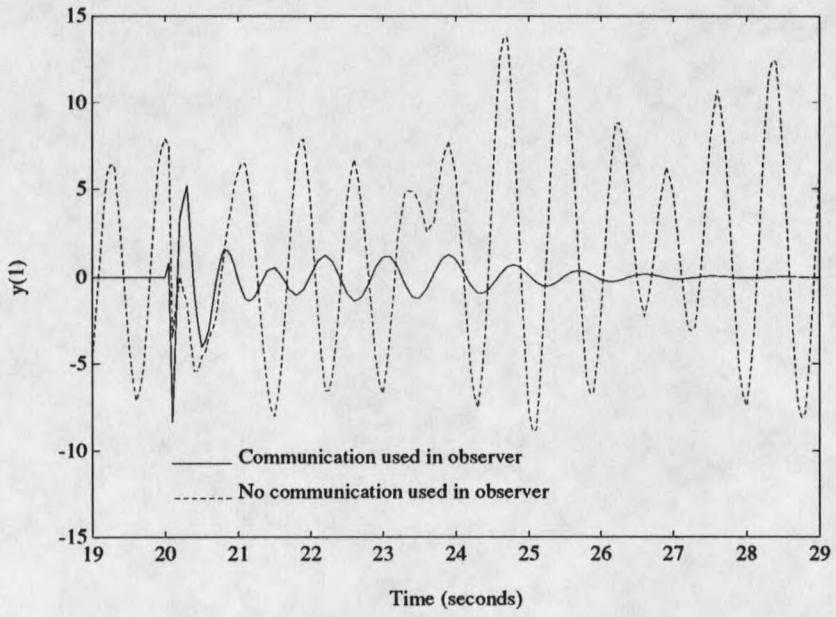

Figure 10. Example 2, closed-loop response of y_1.

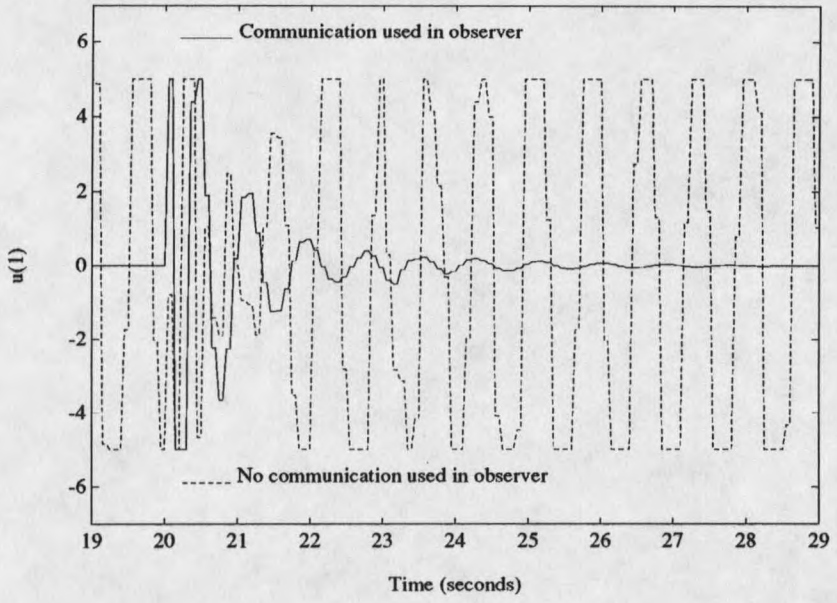

Figure 11. Example 2, closed-loop response of u_1.

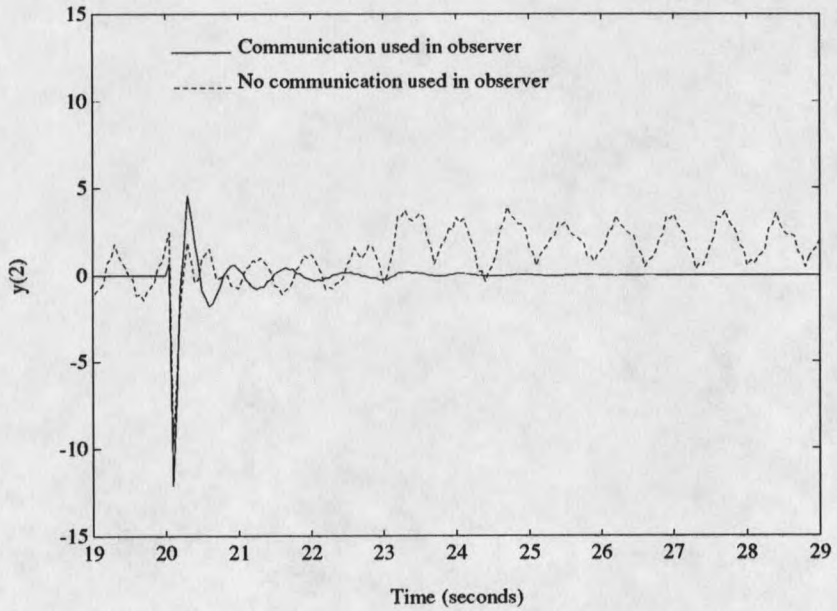

Figure 12. Example 2, closed-loop response of y_2.

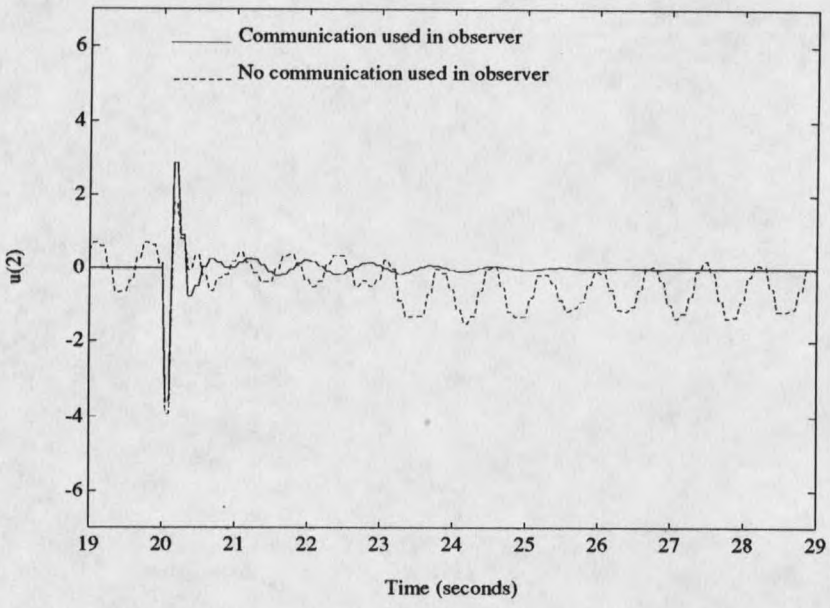

Figure 13. Example 2, closed-loop response of u_2.

Example 3

Many of the adaptive control schemes in the literature (both decentralized and centralized) require the observer to be deadbeat. The observer used with the adaptive control scheme proposed in this thesis allows the observer to have its poles arbitrarily placed inside the unit circle. This freedom can be used in a number of ways. This example demonstrates how the observer poles can be placed to obtain a filtering action on the controlled input and reduce the magnitude of initial swings while preserving the system damping.

The system described by (2.67) is again considered. The decentralized adaptive control scheme is applied to the plant. For one case the observer poles are placed at 0.5

and $0.5e^{\pm j30°}$, and for the other the observers are deadbeat. The LQ control laws and identifiers settings are: LQ control laws -- $\omega_{11}=\omega_{12}=10$, $\omega_{21}=\omega_{22}=10$, $\gamma_1=\gamma_2=0.99$; identifiers -- $\lambda_1=\lambda_2=0.97$.

The same disturbance used in previous examples is applied to the plant. Figures 14 and 15 show y_1 and u_1 for both observer cases, and the y_2 and u_2 are shown in Figures 16 and 17.

The nondeadbeat observer results in a better initial system response. The response is better because the initial system overshoot is significantly decreased. Also, the controlled inputs are much "smoother," and do not saturate.

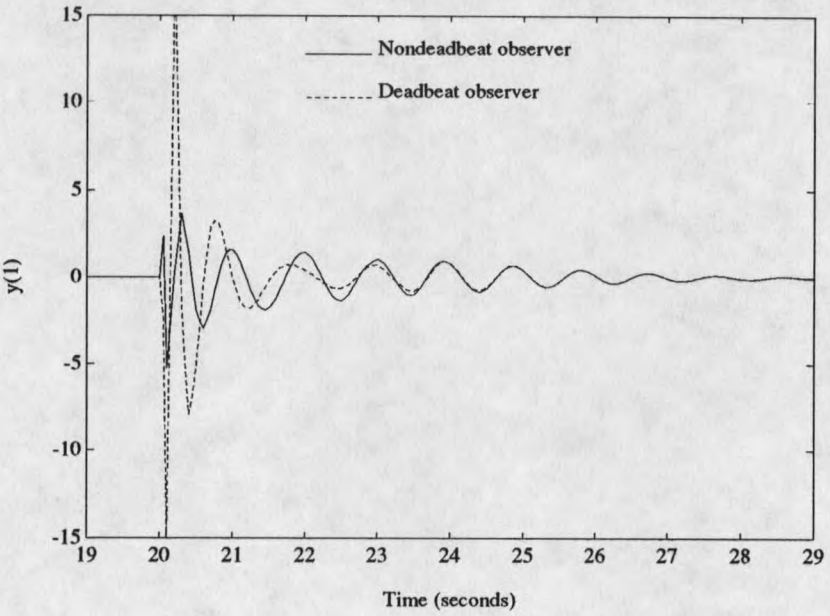

Figure 14. Example 3, closed-loop response of y_1.

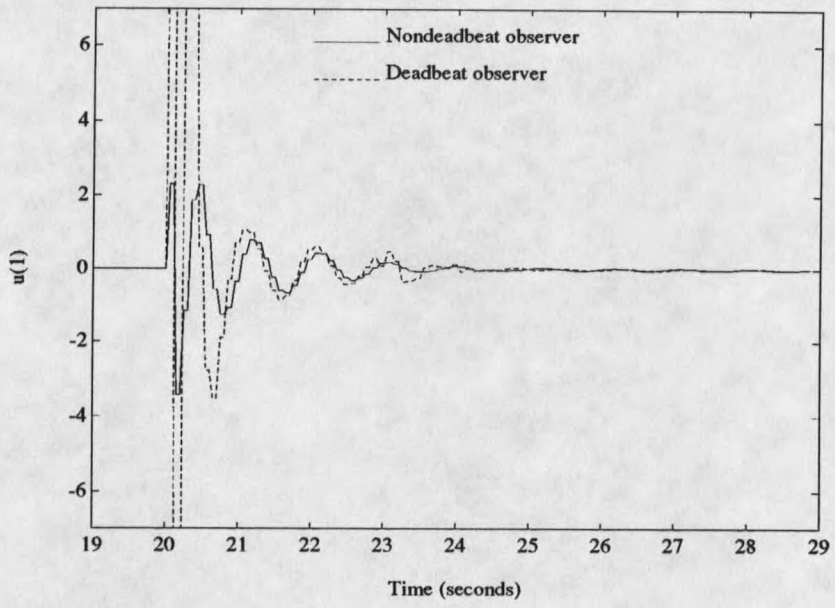

Figure 15. Example 3, closed-loop response of u_1.

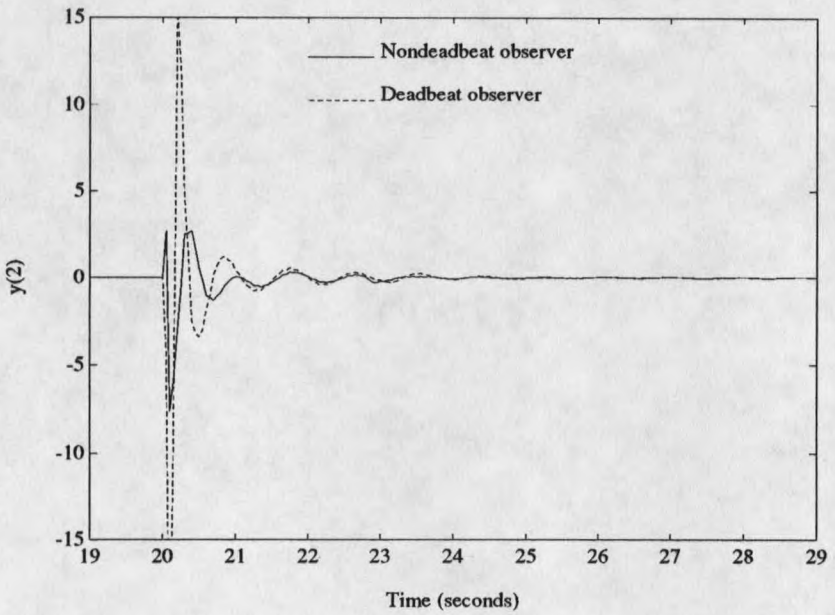

Figure 16. Example 3, closed-loop response of y_2.

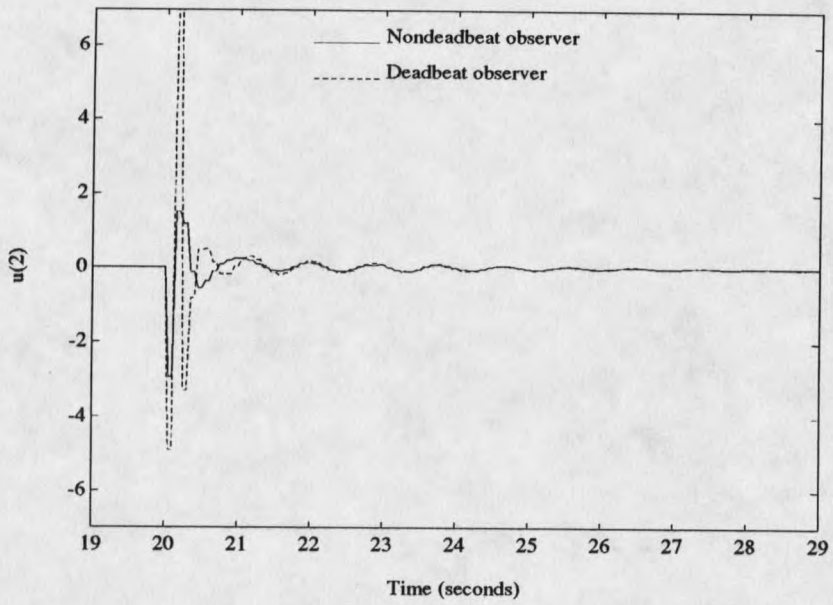

Figure 17. Example 3, closed-loop response of u_2.

Example 4

By studying Theorem 2.1 and Corollary 2.1, one can see that the larger the subsystem interconnections and the larger the feedback gains the more critical communication is between control stations. In this example it is demonstrated that when subsystem interconnections are weak, less is gained from the use of communication.

Consider the system

$$\dot{x}_1 = \begin{bmatrix} 0 & 1 \\ -4\pi^2 & 0 \end{bmatrix} x_1 + \begin{bmatrix} 0 \\ 8 \end{bmatrix} u_1$$

$$\dot{x}_2 = \begin{bmatrix} 0 & 1 \\ -0.64\pi^2 & 0.1 \end{bmatrix} x_2 + \begin{bmatrix} 0 \\ -0.7 \end{bmatrix} u_1 + \begin{bmatrix} 0.8 \\ 0 \end{bmatrix} u_2 \qquad (2.68)$$

$$\dot{x}_3 = \begin{bmatrix} 0 & 1 \\ -5\pi^2 & 0 \end{bmatrix} x_3 + \begin{bmatrix} 0 \\ 9 \end{bmatrix} u_2$$

$$y_1 = [5 \quad 0]x_1 + [0.6 \quad 0]x_2$$

$$y_2 = [0.7 \quad 0]x_2 + [9 \quad 0]x_3$$

which is the same as (2.67) except the subsystem interconnection terms have been reduced by one-tenth.

Two control cases are considered for this example. As with Example 1, one case is the control scheme that uses communicated information while the other uses independent adaptive controllers with no communication between controllers. The identifiers, observers, and LQ control laws for both cases have the following settings: LQ control laws -- $\omega_{11}=\omega_{12}=100$, $\omega_{21}=\omega_{22}=200$, $\gamma_1=\gamma_2=0.99$; both local observers are designed to have poles at 0.5 and $0.5e^{\pm j30^\circ}$; identifiers -- $\lambda_1=\lambda_2=0.97$. Because the ω_{i1}'s and ω_{i2}'s are much larger for this example than in Example 1, it is expected the magnitude of the feedback gains will be smaller.

The disturbance used in Example 1 is used here. Figures 18 and 19 show open-loop system response. The closed-loop system response is shown in Figures 20 and 21. In contrast to the results in Example 1, there is little difference between the communicated and the no communicated controller cases. This example along with Example 1 demonstrate that use of communications between control stations may only be needed when the subsystem interconnections are large.

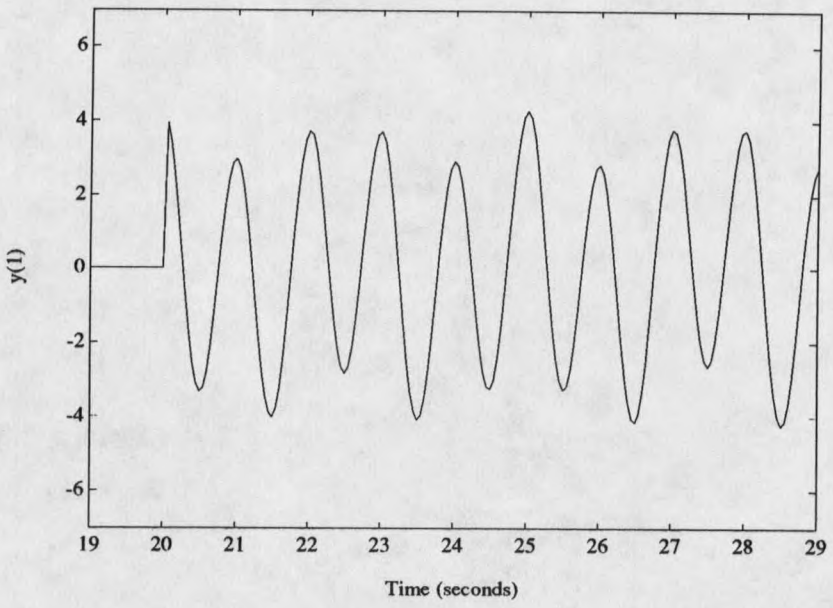

Figure 18. Example 4, open-loop response of y_1.

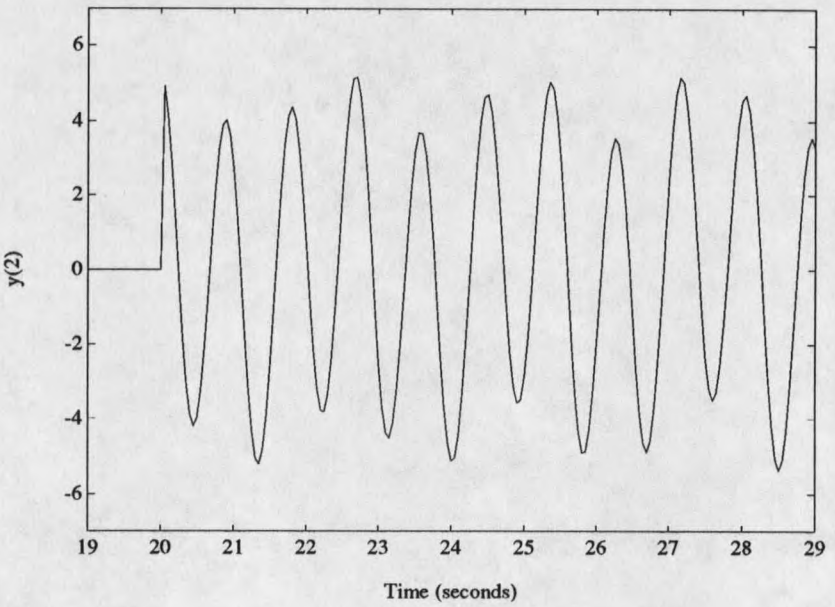

Figure 19. Example 4, open-loop response of y_2.

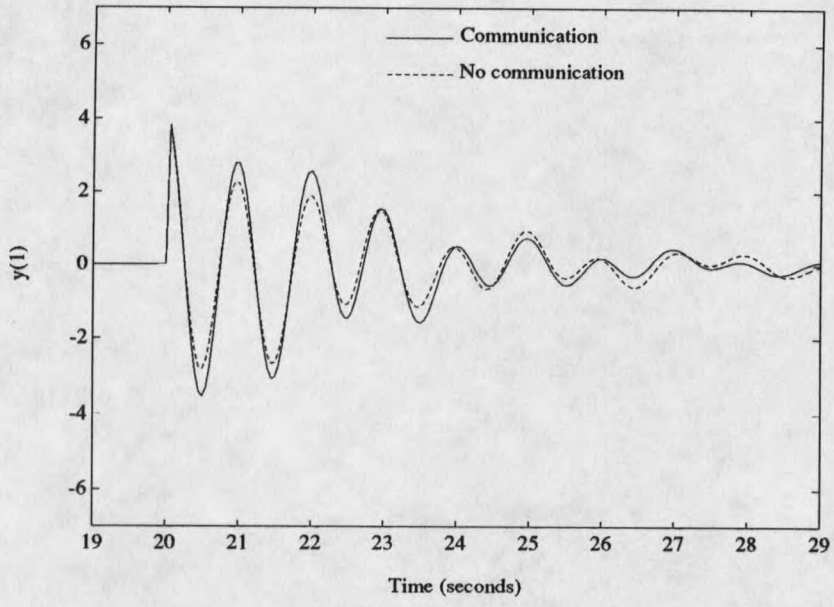

Figure 20. Example 4, closed-loop response of y_1.

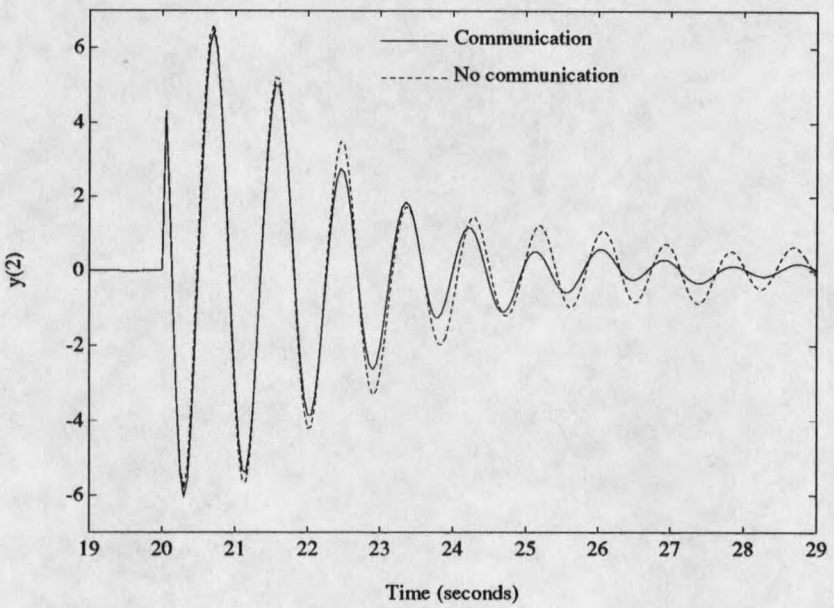

Figure 21. Example 4, closed-loop response of y_2.

Example 5

In this example the effect of the γ_i term in the Riccati and gain equations (2.12) is demonstrated. It was discussed earlier that the LQ control law is one that will minimize the cost function (2.14). The constant γ_i forces the local closed-loop system to have all its poles inside a circle of radius γ_i. If the objective is to dampen an oscillatory system, as with the power system problem, then a $\gamma_i < 1$ may be required.

Consider the discrete-time system

$$\frac{y(z)}{u(z)} = \frac{(z - 0.9454 \pm j0.3259)}{(z - 0.8092 \pm j0.5876)(z - 0.9509 \pm j0.3096)} \tag{2.69}$$

where the "$\pm$" denotes two complex conjugate pairs multiplied together. System (2.69) is a two oscillator system with two sets of poles on the unit circle, and it is both controllable and observable. The system is placed in observable canonical form and a nonadaptive LQ controller is designed for two cases. The LQ controller settings are: $\omega_{i1}=\omega_{i2}=10$; for one case, $\gamma_i=1.0$; for the other case, $\gamma_i=0.9$.

In the $\gamma_i=1$ case the steady-state solution to the Riccati and gain equations (2.12) are $k_i^T=$[0.4852 0.2677 0.1133 0.0453] and $\alpha_i=0.0339$. The closed-loop transfer function is

$$\frac{y(z)}{u(z)} = \frac{z(z - 0.9454 \pm j0.3259)}{(z - 0.23)(z - 0.1004 \pm j0.3711)(z - 0.9443 \pm j0.3254)} \tag{2.70}$$

The closed-loop (2.70) has a pole pair very close to the unit circle (a magnitude of 0.999). This pole pair is very nearly cancelled by a pair of system zeros. Instead of the LQ controller moving the poles well inside the unit circle as one might expect, it moved one pair of poles very close to system zeros. This is acceptable to the LQ controller as the only guarantees the controller gives is that the closed-loop poles are inside the unit circle and the cost (2.14) is minimized. This near pole/zero cancellation is not unique to this system or choice of weights as it occurs for many oscillatory systems and for a wide range of ω_{i1}'s and ω_{i2}'s.

With the γ_i=0.9 case the steady-state gains are k_i^T=[3.9986 5.6159 6.7802 7.3355] and α_i=0.0153, and the closed-loop system is

$$\frac{y(z)}{u(z)} = \frac{z(z-0.9454 \pm j0.3259)}{(z-0.2067)(z-0.0796 \pm j0.3267)(z-0.7649 \pm j0.2641)} \qquad (2.71)$$

All the poles of (2.70) are inside a circle of radius 0.9. Having γ_i=0.9 did not allow the LQ controller to use a pole/zero cancellation near the unit circle to minimize the cost function.

CHAPTER 3

SYSTEM IDENTIFICATION USING PRONY ANALYSIS

The majority of feedback design techniques developed from modern control theory are based on a linear time-invariant mathematical model of the plant. Many plants (such as large power systems) are actually nonlinear, time varying, and of an extremely large order. In order to design controllers for such systems, reduced- order linear models are often used to represent the plant operating near a given equilibrium point. Because of the complexity and size of many systems, it is often very difficult to obtain an accurate model based on the laws of physics. An alternative to using the laws of physics is to use a system identification method based on system input/output data. Presented in this chapter is a method of obtaining accurate reduced-order models of large plants.

The method is an off-line technique in that a number of data points are analyzed together as opposed to a recursive technique where the model is updated with each new data sample. The system identification method is based on Prony signal analysis. With the technique, a known input of a given class is applied to the system and the output is analyzed using Prony signal analysis. An optimal linear

model of the system is obtained by combining the Prony analysis results and the knowledge of the input. The linear model is optimal in the least-squares sense.

Prony analysis is an off-line signal analysis technique that fits a weighted summation of damped modal components in the form

$$\hat{y}(t) = \sum_{i=1}^{n} B_i e^{\lambda_i t} \tag{3.1}$$

to a given signal $y(t)$, where $B_i \in C$ is the signal or output residue associated with the ith eigenvalue $\lambda_i \in C$, and the λ_i's are distinct. Both $y(t)$ and $\hat{y}(t)$ are real valued functions of t. The λ_i's and B_i's are obtained by fitting $\hat{y}(t)$ to $y(t)$ in a least-squared-error sense. Prony analysis is well suited for identifying signals of large order, and it can be modified to give an estimate of the signal order.

Recently, work has been presented by Hauer, et al., in [44] and [45], which uses Prony analysis to analyze power system electromechanical oscillations. The results of Hauer's work indicate that Prony analysis is well suited for the type of signals present in a power system. In Chapter 4 the Prony based system identification method presented here, which is an extension of that presented in [60], is used to design PSS units for a simulated power system. It is important to note that conventional Prony analysis identifies a model of a signal; it does not identify a system model.

The six main sections of this chapter that follow include: 1) a discussion of the Prony signal analysis technique; 2) a presentation of the system identification method; 3) a procedure for obtaining an estimate of the system order; 4) criteria for choosing the input signal with the system identification method; 5) a discussion of the numerical problems that must be solved when programing the system identification method; and 6) an example.

Prony Signal Analysis

Prony signal analysis is a method of analyzing signals to determine modal, damping, phase, and magnitude information contained in the signal. It originated nearly 200 years ago [46], but only with the advancement of the digital computer has it been extensively used. A sample of recent work is contained in [44], [45], and [47]-[50]. One well established use of Prony analysis is in the design of digital filters as described in [47]. In this section the standard Prony signal analysis method is described. A similar presentations is contained in [48].

Consider a general signal $y(t)$ that is to be modeled by $\hat{y}(t)$ which is described by (3.1). The signal $y(t)$ is sampled at a sample period (T_s) smaller than the Nyquist period, resulting in the sequence $y_k \equiv y(kT_s)$, $k = 0, 1, \ldots, N-1$. With $t = kT_s$, the discrete form of $\hat{y}(t)$ is $\hat{y}_k \equiv \hat{y}(kT_s)$, and from (3.1),

$$\hat{y}_k = \sum_{i=1}^{n} B_i z_i^k; \quad k = 0, 1, \ldots, N-1 \tag{3.2}$$

where B_i is the output residue in (3.1) and

$$z_i = e^{\lambda_i T_s} \tag{3.3}$$

The z_i's are termed the discrete-time eigenvalues. The ideal objective is to find the B_i's, λ_i's, and n that produce $\hat{y}_k = y_k$, $k = 0, 1, \ldots, N-1$. To satisfy this ideal objective requires that n be related to N, but in most cases this is unrealistic (especially since n is assumed to be unknown). A more realistic objective is to find the B_i's, λ_i's, and n that result in $\hat{y}_k$ being the best fit to y_k in a least-squares sense. This is the objective that Prony analysis satisfies.

Assume that $N > 2n$; also assume, for the time being, that n is known. Equations (3.2) are expanded and equated to y_k resulting in

$$\begin{bmatrix} z_1^0 & z_2^0 & \cdots & z_n^0 \\ z_1^1 & z_2^1 & \cdots & z_n^1 \\ \cdot & \cdot & & \cdot \\ \cdot & \cdot & & \cdot \\ \cdot & \cdot & & \cdot \\ z_1^{N-1} & z_2^{N-1} & \cdots & z_n^{N-1} \end{bmatrix} \begin{bmatrix} B_1 \\ B_2 \\ \cdot \\ \cdot \\ \cdot \\ B_n \end{bmatrix} = \begin{bmatrix} y_0 \\ y_1 \\ \cdot \\ \cdot \\ \cdot \\ y_{N-1} \end{bmatrix} \tag{3.4a}$$

or in a compact form

$$ZB = Y \tag{3.4b}$$

where $Z \in C^{Nxn}$, $B \in C^n$, and $Y \in \Re^N$. System (3.4) is an over-determined set of equations. If the z_i's were known, then a least-squares solution of (3.4) could be solved to obtain the optimal B_i's.

It is well known that the discrete-time eigenvalues are the roots of the characteristic equation. Let $a_i \in \Re$, $i = 1,2,...,n$ be coefficients of the characteristic polynomial where

$$z_i^n - (a_1 z_i^{n-1} + a_2 z_i^{n-2} + ... + a_n) = 0; \quad i = 1,2,...,n \tag{3.5}$$

and define $\overline{a}_i \in \Re^N$ as

$$\overline{a}_i \equiv [(i \quad 0's) \quad -a_n \quad -a_{n-1} \quad ... \quad -a_1 \quad 1 \quad (N-n-i-1 \quad 0's)]^T \tag{3.6}$$

for $i = 0,1,...,N-n-1$. Multiply both sides of (3.4) by $\overline{a}_i^T$ to obtain

$$\overline{a}_i^T Y = \overline{a}_i^T Z B; \quad i = 0,1,...,N-n-1 \tag{3.7}$$

From (3.5), $\overline{a}_i^T Z = 0$; therefore,

$$\overline{a}_i^T Y = 0; \quad i = 0,1,...,N-n-1 \tag{3.8}$$

Equations (3.8) can also be written as

$$-a_n y_i - a_{n-1} y_{i+1} - ... - a_1 y_{n+i-1} + y_{n+i} = 0 \tag{3.9}$$

for $i = 0,1,...,N-n-1$, or in matrix form as

$$\begin{bmatrix} y_0 & y_1 & \cdots & y_{n-1} \\ y_1 & y_2 & \cdots & y_n \\ \cdot & \cdot & & \cdot \\ \cdot & \cdot & & \cdot \\ \cdot & \cdot & & \cdot \\ y_{N-n-1} & y_{N-n} & \cdots & y_{N-2} \end{bmatrix} \begin{bmatrix} a_n \\ a_{n-1} \\ \cdot \\ \cdot \\ \cdot \\ a_1 \end{bmatrix} = \begin{bmatrix} y_n \\ y_{n+1} \\ \cdot \\ \cdot \\ \cdot \\ y_{N-1} \end{bmatrix} \tag{3.10}$$

which is also a set of over-determined equations.

Prony analysis involves four steps. The first step is to solve (3.10) for the a_i's that give the optimal least-squares solution to this set of over-determined equations. Second, (3.5) is factored to obtain the discrete-time eigenvalues (the z_i's). The third step involves solving (3.4) for the B_i's (in a least-squares sense). Lastly, (3.3) is solved for the λ_i's.

System Identification using Prony Analysis

Prony analysis is a signal identification technique, not a system identification method. Because standard Prony signal analysis does not use knowledge of the system input, it cannot identify a model for a system. But, as shown in this section, if the input is restricted to be of a certain class and knowledge of the input is used in the analysis, then a system model can be obtained using Prony analysis.

Consider a general system with input $u(t)$ and output $y(t)$. It is desired to obtain a linear system model. The Laplace domain of the linear model of the system is denoted by $G(s)$; a block diagram of the linear model is shown in Fig-

ure 22. $U(s)$, the Laplace transform of $u(t)$, is the input applied to both the system and the model, and $\hat{Y}(s)$ is the output of the model. $W(s)$ represents a model for any non-zero initial conditions present in the system. The objective is to find both the $G(s)$ and the $W(s)$ that result in $\hat{y}(t)$ being a least-squares fit to $y(t)$, where $\hat{y}(t)$ is the inverse Laplace transform of $\hat{Y}(s)$.

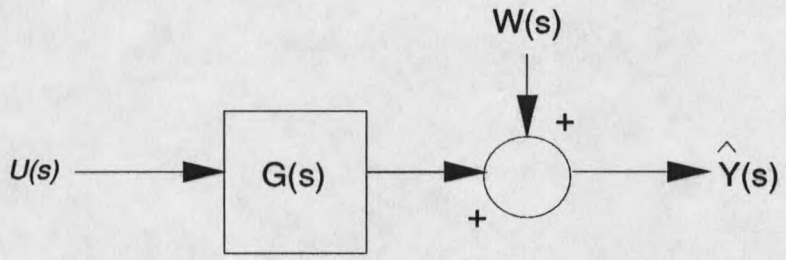

Figure 22. System model with initial conditions.

Assume $G(s)$ is of the form

$$G(s) = e^{-sD'} \sum_{i=1}^{n} \frac{R_i}{s - \lambda_i} \tag{3.11}$$

where $D' \in \Re$ is a known pure system time delay, $R_i \in C$ is the transfer-function residue associated with the ith eigenvalue λ_i, and the λ_i's are assumed to be distinct.

The input is restricted to a series of time delayed signals all with the same eigenvalue. The Laplace transform of the input signal is

$$U(s) = \sum_{j=0}^{q} c_j \frac{e^{-sD_j} - e^{-sD_{j+1}}}{s - \lambda_{n+1}} \tag{3.12}$$

where $\lambda_{n+1} \neq \lambda_i$, $i = 1,2,\ldots,n$, and $D_0 \equiv 0$ without loss of generality. A typical plot of $u(t)$ for the case that $\lambda_{n+1} = 0$ and $q = 3$ is given in Figure 23. The system initial-condition model is

$$W(s) = \sum_{i=1}^{n} \frac{A_i}{s - \lambda_i} \tag{3.13}$$

where $A_i \in C$ is the initial-condition residue associated with ith eigenvalue.

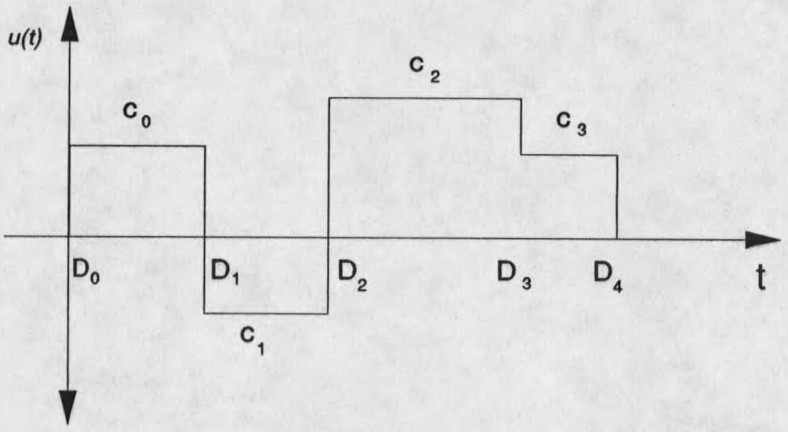

Figure 23. $u(t)$ for the case when $\lambda_{n+1} = 0$ and $q = 3$.

The transform $\hat{Y}(s)$ of the system model output in Figure 22 is

$$\hat{Y}(s) = U(s)G(s) + W(s) \tag{3.14}$$

or from (3.11), (3.12), and (3.13),

$$\hat{Y}(s) = \left(\sum_{j=0}^{q} c_j \left(e^{-sD_j} - e^{-sD_{j+1}} \right) \right) \left(e^{-sD'} \sum_{i=1}^{n} \frac{R_i}{(s - \lambda_i)(s - \lambda_{n+1})} \right) + \sum_{i=1}^{n+1} \frac{A_i}{s - \lambda_i} \tag{3.15}$$

Using partial fraction expansion, (3.15) is

$$\hat{Y}(s)=\left(\sum_{j=0}^{q} c_j\left(e^{-sD_j}-e^{-sD_{j+1}}\right)\right)\left(e^{-sD'}\sum_{i=1}^{n+1}\frac{Q_i}{(s-\lambda_i)}\right)+\sum_{i=1}^{n+1}\frac{A_i}{s-\lambda_i} \tag{3.16}$$

where

$$Q_i \equiv \frac{R_i}{\lambda_i-\lambda_{n+1}};\quad i=1,2,\ldots,n \tag{3.17a}$$

and

$$Q_{n+1} \equiv -\sum_{i=1}^{n} Q_i \tag{3.17b}$$

Equation (3.16) can also be written as

$$\hat{Y}(s)=\sum_{j=0}^{q} c_j\left(\sum_{i=1}^{n+1}\frac{e^{-s(D_j+D')}Q_i}{(s-\lambda_i)}-\sum_{i=1}^{n+1}\frac{e^{-s(D_{j+1}+D')}Q_i}{(s-\lambda_i)}\right)+\sum_{i=1}^{n+1}\frac{A_i}{s-\lambda_i} \tag{3.18}$$

The inverse Laplace transform of (3.18) is

$$\hat{y}(t)=\sum_{j=0}^{q} c_j\sum_{i=1}^{n+1} Q_i\left(e^{\lambda_i(t-D_j-D')}\mu(t-D_j-D')-e^{\lambda_i(t-D_{j+1}-D')}\mu(t-D_{j+1}-D')\right)$$
$$+\sum_{i=1}^{n+1} A_i e^{\lambda_i t} \tag{3.19}$$

where $\mu(\cdot)$ denotes the unit step function. Equation (3.19) can also be written as

$$\hat{y}(t)=\sum_{i=1}^{n+1}\left[A_i+e^{-\lambda_i D'}Q_i\sum_{j=0}^{q} c_j\left(e^{-\lambda_i D_j}\mu(t-D_j-D')-e^{-\lambda_i D_{j+1}}\mu(t-D_{j+1}-D')\right)\right]e^{\lambda_i t} \tag{3.20}$$

Two cases are of interest when obtaining a system model. With the first case, it is assumed that $A_i \equiv 0$, $i=1,2,\ldots,n+1$. For the second case, A_i is not necessarily zero. When $A_i \equiv 0$ only one Prony analysis needs to be done on the data to obtain a model. With the second case, two analyses are performed over two different sets of data.

The following two subsections show why this is true and develop the equations that can be solved to obtain the system model.

Case 1: Zero Initial Conditions

With $A_i \equiv 0$ and $t \geq D_{q+1} + D'$, output (3.20) can be written as

$$\hat{y}(t) = \sum_{i=1}^{n+1} \left[e^{-\lambda_i D'} Q_i \sum_{j=0}^{q} c_j \left(e^{-\lambda_i D_j} - e^{-\lambda_i D_{j+1}} \right) \right] e^{\lambda_i t}, \quad t \geq D_{q+1} + D' \tag{3.21}$$

Let $\tau \equiv t - D_{q+1} - D'$, and define

$$\hat{v}(\tau) \equiv \hat{y}(\tau + D_{q+1} + D') \tag{3.22}$$

which can also be written as

$$\hat{v}(\tau) = \sum_{i=1}^{n+1} B_i e^{\lambda_i \tau}, \quad \tau \geq 0 \tag{3.23}$$

where

$$B_i = Q_i \sum_{j=0}^{q} c_j \left(e^{\lambda_i (D_{q+1} - D_j)} - e^{\lambda_i (D_{q+1} - D_{j+1})} \right); \quad i = 1, 2, \ldots, n+1 \tag{3.24}$$

which is solved for Q_i:

$$Q_i = \frac{B_i}{c_0 e^{\lambda_i D_{q+1}} - c_q + \sum_{j=1}^{q} (c_j - c_{j-1}) e^{\lambda_i (D_{q+1} - D_j)}}; \quad i = 1, 2, \ldots, n+1 \tag{3.25}$$

and the transfer-function residues are obtained by combining (3.17a) and (3.25) to obtain

$$R_i = \frac{B_i (\lambda_i - \lambda_{n+1})}{c_0 e^{\lambda_i (D_{q+1} - D_0)} - c_q + \sum_{j=1}^{q} (c_j - c_{j-1}) e^{\lambda_i (D_{q+1} - D_j)}}; \quad i = 1, 2, \ldots, n \tag{3.26}$$

The B_i and λ_i terms in (3.26) are obtained by performing a Prony analysis on (3.23). The c_j, D_j and λ_{n+1} terms are known from the input, and D' is known. Therefore, assuming the system initial conditions are zero, a least-squared-error model of the system is obtained by: 1) applying an input of the form of (3.12) to the system; 2) forming a delayed version of the corresponding output ($v(\tau)$); 3) performing a Prony analysis on $v(\tau)$ to obtain eigenvalues and output residues; and 4) solving (3.26) for the transfer-function residues.

Case 2: Nonzero Initial Conditions

In this case the objective is not only to obtain a model of the system but to acquire a model of the system initial conditions. That is, the objective is obtain estimates for $G(s)$ and $W(s)$ in (3.11) and (3.13), respectively.

For $D'+D_m \le t < D'+D_{m+1}$, (3.20) may be written as

$$\hat{y}(t) = \sum_{i=1}^{n+1}\left[A_i + e^{-\lambda_i(D'+D_m)}Q_i c_m + e^{-\lambda_i D'}Q_i \sum_{j=0}^{m-1} c_j\left(e^{-\lambda_i D_j} - e^{-\lambda_i D_{j+1}}\right)\right]e^{\lambda_i t} \qquad (3.27)$$

Similar to case 1, we define $\tau \equiv t - D_m - D'$ and

$$v_m(\tau) \equiv \hat{y}(\tau + D' + D_m) \qquad (3.28)$$

$$= \sum_{i=1}^{n+1} B_i^m e^{\lambda_i \tau}, \quad 0 \le \tau < D_{m+1} - D_m \qquad (3.29)$$

in which the B_i^m coefficients are identified from (3.27) as

$$B_i^m = A_i e^{\lambda_i(D'+D_m)} + Q_i\left\{c_m + \sum_{j=0}^{m-1} c_j\left[e^{\lambda_i(D_m - D_j)} - e^{\lambda_i(D_m - D_{j+1})}\right]\right\} \qquad (3.30)$$

for $i=1,2,\ldots,n+1$. Note that one application of Prony analysis can be used to obtain the B_i^m's, but that the unknowns in (3.30) are then A_i and Q_i. In order to solve for these unknowns, a second Prony analysis is conducted over a later time interval, say from $t=D'+D_p$ to $t=D'+D_{p+1}$, in the same manner as before, to obtain a second set of B_i's, in this case,

$$B_i^p = A_i e^{\lambda_i(D'+D_p)} + Q_i\left\{c_p + \sum_{j=0}^{p-1} c_j\left[e^{\lambda_i(D_p-D_j)} - e^{\lambda_i(D_p-D_{j+1})}\right]\right\} \tag{3.31}$$

Equations (3.30) and (3.31) are solved by multiplying (3.30) by $e^{\lambda_i(D_p-D_m)}$, subtracting it from (3.31), and solving for Q_i:

$$Q_i = \frac{B_i^p - B_i^m e^{\lambda_i(D_p-D_m)}}{\sum_{j=m+1}^{p}(c_j-c_{j-1})e^{\lambda_i(D_p-D_j)}} \tag{3.32}$$

where it is assumed that $p>m$. With Q_i available from (3.32), the transfer-function residue R_i follows from (3.17a) as

$$R_i = \frac{(\lambda_i-\lambda_{n+1})\left(B_i^p - B_i^m e^{\lambda_i(D_p-D_m)}\right)}{\sum_{j=m+1}^{p}(c_j-c_{j-1})e^{\lambda_i(D_p-D_j)}} \tag{3.33}$$

and A_i follows from (3.30) as

$$A_i = e^{-\lambda_i(D'+D_m)}B_i^m - e^{-\lambda_i D'}Q_i\left[c_0 + \sum_{j=1}^{m}(c_j-c_{j-1})e^{-\lambda_i D_j}\right] \tag{3.34}$$

Thus, two applications of the Prony method, applied to the same transient but over distinct time intervals, are used to estimate both the transfer-function residues and the initial conditions associated with the transient.

In the above derivation it is implicitly assumed that $p < q+1$. This is not a necessary requirement. It can easily be shown that if $p = q+1$ with $c_{q+1} \equiv 0$, the same solution (i.e., equations (3.33) and (3.34)) results.

The method of obtaining a system model is summarized in the following steps: 1) an input of the form of (3.12) is applied to the system; 2) two delayed signals are obtained from the output corresponding to (3.28), one for m and one for p; 3) a Prony analysis is conducted on both delayed signals and the system eigenvalues and output residues are obtained; 4) (3.33) and (3.34) are solved for the transfer-function and initial-condition residues. In step 3 it is assumed that each Prony analysis results in the same eigenvalues; in some cases this may not occur. Therefore, when the two analysis are carried out, one must make sure that each Prony analysis results in the same eigenvalues. It is possible to use the eigenvalues from one analysis in the other, or a combination of eigenvalues could be used.

Estimating the System Order

It was previously mentioned that the objective of the Prony based system identification method is to estimate a

model for a system including the order of the model (n). Up to this point, it has been assumed that n is known. In this section a method of estimating n is given. The method is based on that given by Kumaresan, et al., in [49]. The method outlined in [49] is used to find the order of a signal model but is easily applicable to the problem of finding a system order.

The method used here to find the system order n is outlined by the following steps:

1. Estimate an upper bound (n_u) for the system order n, where $n_u \geq n$.
2. Perform a Prony based analysis on the data using n_u as the order of the model in (3.11). This results in n_u residue/eigenvalue terms (i.e. (R_i, λ_i), $i = 1, 2, \ldots, n_u$) which are candidates for the system model components.
3. Use a search technique based on that of Hocking and Leslie [51] to obtain the smallest subset of the n_u residue/eigenvalue terms that accurately fit the data. This subset is the system model, and the order of the subset is the estimated n.

Deciding on an upper bound n_u is not done arbitrarily. It is recommended in [50] that when singular-value decomposition is used to solve the over-determined systems, n_u

should be between $N/3$ and $N/2$. This results in the most accurate solution to the least-squares-error problem in the presence of Gaussian noise.

The Hocking and Leslie search technique starts by applying the input $u(t)$ to the n_u transfer functions

$$e^{-sD'}\frac{R_i}{s-\lambda_i};\quad i=1,2,\ldots,n_u \tag{3.35}$$

resulting in n_u outputs (i.e., n_u $\hat{y}'$s). The one (R_i,λ_i) pair from (3.35) resulting in the $\hat{y}$ that minimizes the error

$$E_i = 20\log_{10}\left[\frac{\sum_{k=0}^{N-1}(y_k-\hat{y}_k)^2}{\sum_{k=0}^{N-1}y_k^2}\right]^{1/2} \tag{3.36}$$

is termed (R_{j_1},λ_{j_1}) and the corresponding error E_1.

After (R_{j_1},λ_{j_1}) and E_1 have been determined, $u(t)$ is applied to the n_u-1 transfer functions

$$e^{-sD'}\left[\frac{R_{j_1}}{s-\lambda_{j_1}}+\frac{R_i}{s-\lambda_i}\right];\quad i=1,2,\ldots,n_u;\quad i\neq j_1 \tag{3.37}$$

resulting in n_u-1 $\hat{y}'$s. The one (R_i,λ_i) from (3.37) resulting in the $\hat{y}$ that minimizes (3.36) is termed (R_{j_2},λ_{j_2}) and the corresponding error E_2.

Now the n_u-2 transfer functions

$$e^{-sD'}\left[\frac{R_{j_1}}{s-\lambda_{j_1}}+\frac{R_{j_2}}{s-\lambda_{j_2}}+\frac{R_i}{s-\lambda_i}\right];\quad i=1,2,\ldots,n_u;\quad i\neq j_1,\quad i\neq j_2 \tag{3.38}$$

are tested to determine the one (R_i, λ_i) that results in (3.36) being minimized. This pair is termed (R_{j_3}, λ_{j_3}) and the corresponding error is E_3. The process is continued until the n_u residue/eigenvalue pairs have been reordered as (R_{j_r}, λ_{j_r}), $r = 1, 2, \ldots, n_u$.

The model order n is determined by studying the errors E_r, $r = 1, 2, \ldots, n_u$. With the addition of each (R_{j_r}, λ_{j_r}), E_r decreases from E_{r-1}. The model order n is taken to be the point where E_r no longer significantly decreases (i.e., n equals the r where E_r stops decreasing). The system model is then

$$e^{-sD'} \sum_{r=1}^{n} \frac{R_{j_r}}{s - \lambda_{j_r}} \tag{3.39}$$

Determining the point where E_r stops decreasing is in many cases obvious (as will be shown in an example later in this chapter). But this may not always be the situation. In any case, determining this point is an engineering judgement that depends on the particular problem being studied.

Choosing the Input

Equation (3.12) allows a considerable amount of flexibility when choosing the system input. In order to obtain an accurate system model, the input should satisfy certain criteria. These criteria are discussed in this section.

It is important that $\lambda_{n+1} \neq \lambda_i$, $i = 1,2,...,n$. In some cases these criteria may be difficult to satisfy since the system eigenvalues are unknown. Filtering the system output can be used to remove any possible λ_{n+1} components from the system. This is what is done when applying the system identification method to a power system in Chapter 4. DC components are filtered from the output, and an input with $\lambda_{n+1} = 0$ is used.

In order to obtain an accurate model of the system, the input must sufficiently excite the system eigenvalues. This is done by making the input signal have relatively large frequency content in the bandwidth of the system. In the power system case, electromechanical modes to be modeled are in the 0.2 to 3.0 Hz range; therefore, the input should have frequency content in this range.

Another factor that must be considered is the amplitude of the input signal. The amplitude must be large enough to excite the system but small enough so as not to force the system too far away from its equilibrium. Choosing the amplitude often boils down to engineering judgement.

Programming the Prony Analysis Method

A FORTRAN computer package that implements the Prony based identification method was developed. A description and listing of the package is contained in Appendix B. Two numerically intensive techniques had to be included in the

package in order to solve the Prony analysis method. These techniques are the solution of over-determined systems of equations and the factorization of a high-order polynomial. The methods used to solve these two problems in the software package in Appendix B are discussed in this section.

Singular-value decomposition (SVD) is used to solve the two over-determined systems of equations. SVD is a well established and numerically robust method for solving an over-determined system. Let $A \in \Re^{mxn}$ denote an arbitrary matrix; it is known that A can be written as

$$A = U[diag(w_i)]V^T \tag{3.40}$$

where $U \in \Re^{mxn}$ and $V \in \Re^{nxn}$ are unitary matrices; i.e., $U^TU = V^TV = I^n$. $w_i \in \Re$, $i = 1,2,...,n$, are the singular values of A. Equation (3.40) is referred to as the singular-value decomposition of A (see [52] for more details). The optimal solution to the over-determined system $Ax = b$ is

$$x^* = \min_{x \in \Re^n} \| Ax - b \| \tag{3.41a}$$

$$x^* = V[diag(1/w_i)]U^Tb \tag{3.41b}$$

This is discussed in [53]. If A is ill-conditioned, then some of the singular values are small or zero. A way of interpreting this is that the information associated with a small singular value is strongly affected by noise and round-off error [53]. The standard way of handling this is

to let $1/w_i \equiv 0$ for the small w_i's in (3.41b). This, in effect, ignores any information associated with that singular value.

Factoring a matrix into the form of (3.40) is an intensive algorithm that requires a number of advanced numerical techniques (such as Householder reduction and diagonalization by the QR procedure). Although the algorithm is complicated, it is numerically robust and works for almost all matrices [53]. The SVD subroutine used in the package contained in Appendix B is a double-precision LINPACK routine.

The second numerically intensive routine that is used in solving the Prony identification problem is factoring a large-order polynomial. A FORTRAN 77 subroutine called QPOLYRT is used to factor the polynomial with the package in Appendix B. QPOLYRT is a quad-precision root-finding routine obtained through the Bonneville Power Administration (BPA), Portland, Oregon. The subroutine has been thoroughly tested by BPA and performs very well.

An Example

Consider the system transfer function

$$G_a(s) = \frac{2-j}{s+0.05-j1.5} + \frac{2+j}{s+0.05+j1.5} + \frac{3}{s+2} \qquad (3.42a)$$

with initial conditions

$$W_a(s) = \frac{0.3 - j0.2}{s + 0.05 - j1.5} + \frac{0.3 + j0.2}{s + 0.05 + j1.5} + \frac{1}{s + 2} \qquad (3.42b)$$

The input $0.5(\mu(t) - \mu(t-1)) + 0.25(\mu(t-6) - \mu(t-6.5))$ which can easily be described by (3.12) is applied to (3.42); the resulting output is shown in Figure 24. The output is sampled at a period of 0.25 seconds, and the input/output data is analyzed using the Prony system identification software package described in Appendix B.

The method of estimating the system order described in the third section of this chapter is incorporated into the identification package in Appendix B. The residue/eigenvalue pairs from the identification package are organized in the order of decreasing errors, where the errors correspond to (3.36). Figure 25 shows the error between the system output and the model output for various system orders. Note that the error does not decrease any further after $n = 3$. This indicates the system is third order, and the first three residue-eigenvalue pairs are included in the model. The resulting model is

$$G(s) = \frac{2.000 - j0.9995}{s + 0.05000 - j1.500} + \frac{2.000 + j0.9995}{s + 0.05000 + j1.500} + \frac{2.999}{s + 2.000} \qquad (3.43a)$$

and the initial-condition model is

$$W(s) = \frac{0.2998 - j0.1999}{s + 0.05000 - j1.500} + \frac{0.2998 + j0.1999}{s + 0.05000 + j1.500} + \frac{0.9998}{s + 2.000} \qquad (3.43b)$$

As can be seen the model $(G(s), W(s))$ is very close to the actual system $(G_a(s), W_a(s))$.

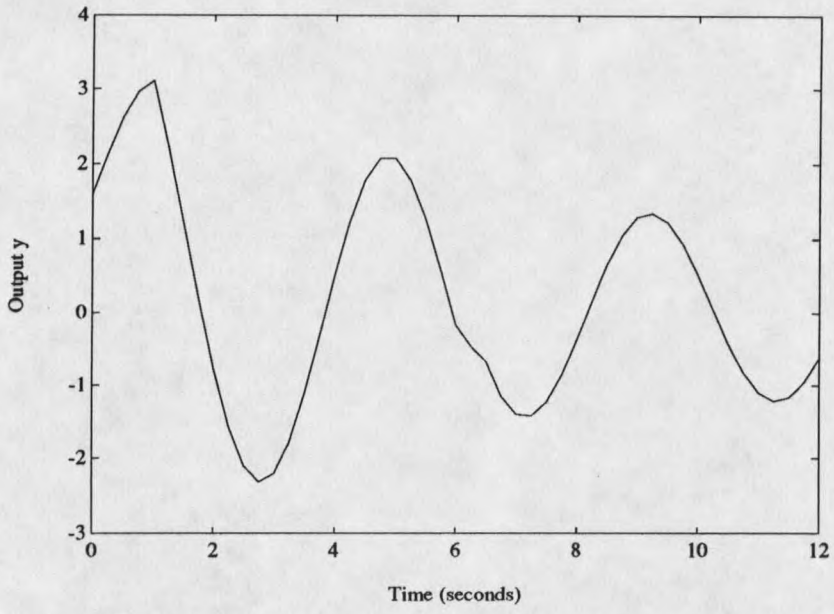

Figure 24. System (3.42) response to the input.

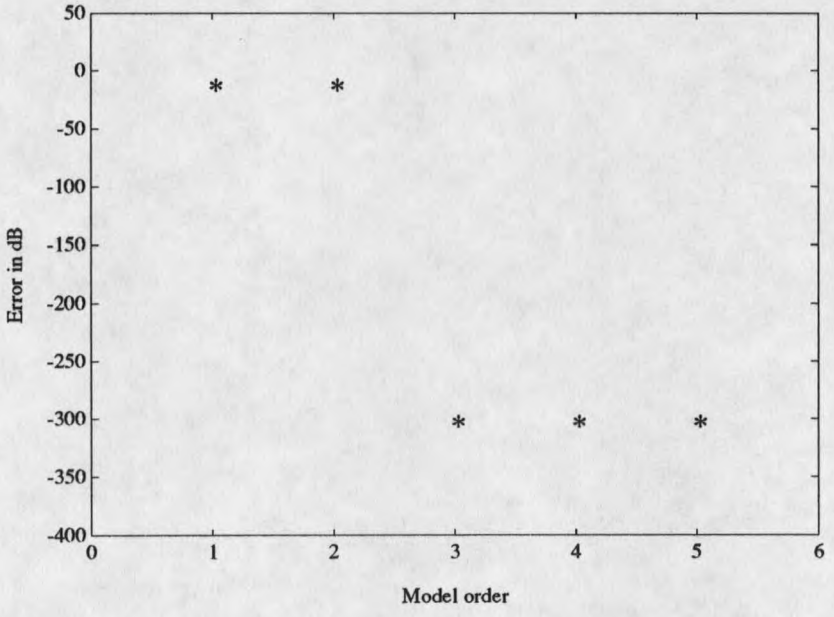

Figure 25. Fitting errors for given model orders.

CHAPTER 4

IMPLEMENTATION OF CONTROLLERS IN A TEST SYSTEM

This chapter is organized into three main sections. In the first section a 17 machine computer-simulated test system is described. This relatively large system (compared to others in the literature) is used in order to make the system behavior as realistic as possible. In the second section both adaptive and conventional PSS units are designed for four generators in the test system. Implementation of the adaptive PSS units is done using the decentralized scheme in Chapter 2. Conventional PSS units are designed using the identification method of Chapter 3. The conventional design technique is similar to that described in [61]. A discussion of how the controllers are embedded in a power-system simulation program is contained in the third section. The properties of the conventional and adaptive control schemes are compared in Chapter 5.

A 17 Machine Test System

To demonstrate the control schemes proposed in this thesis a 17 machine test system is used. This system was derived to be a low-order model of the western North American power system. A detailed description of the derivation

is contained in [54]. A one line diagram of the test system is shown in Figure 26. The operating condition for this system is denoted as operating point A. The system consists of nine main areas; the names of these areas are: A, C, M, NW1, NW2, P, SC1, SC2, U. Each area consists of a load and a number of machines connected to a main bus. All the transmission lines connecting areas are 500 kV lines except those between areas C-M, M-U, A-U, and U-NW2 which are 230 kV lines (Note: "C-M" denotes the transmission line between areas C and M). All short lines within the areas are at 20 kV as are the generators. Table 1 shows the generation and load in each area.

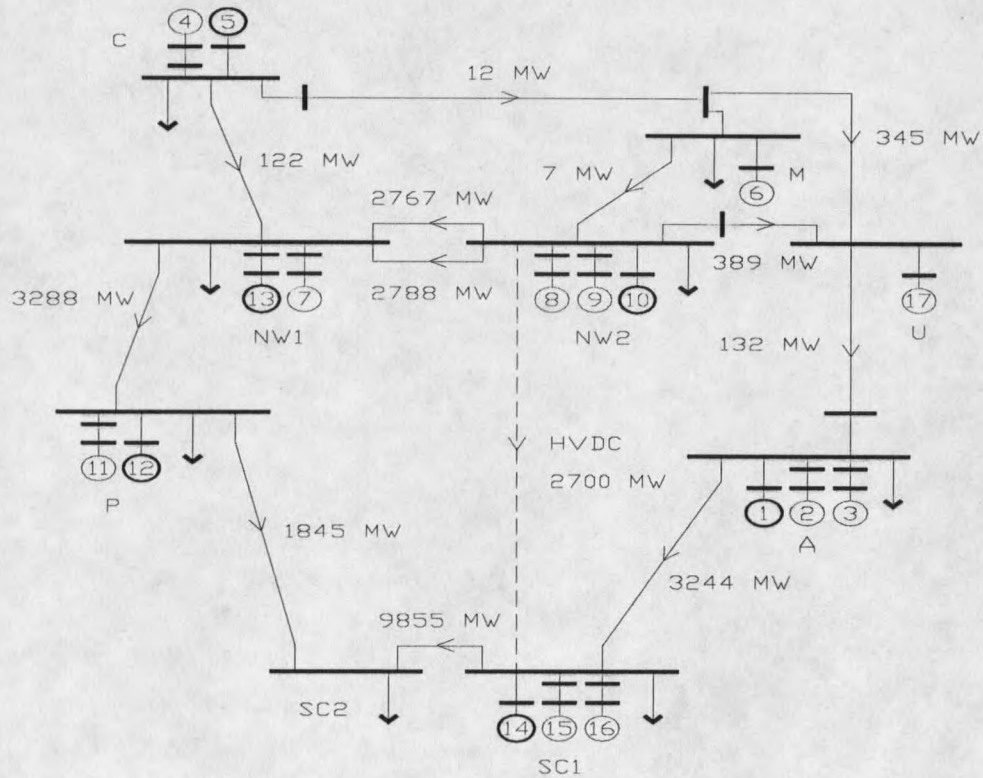

Figure 26. Test system (operating point A).

Area	Generation (MW)	Load (MW)
A	19,000	15,600
C	11,900	11,750
M	1,250	900
NW1	9,169	11,100
NW2	17,700	9,000
P	11,300	12,600
SC1	14,200	9,800
SC2	0	11,700
U	3,200	3,800

Table 1. Generation and load of each area (operating point A).

Two types of generators are modeled in the system. One type of generator has large power generation and inertia. It is meant to represent an aggregate of smaller machines that swing together during a transient. These generators are modeled using classical second-order machine representation with a constant voltage behind a reactance [55]. Heavy circles are used to represent these machines in Figure 26, and they are connected to the main bus in each area by a transformer. The other type of generator is a smaller more-realistic one. Generators of this type are simulated using a two-axis fourth-order nonlinear model, and they have exciters that are modeled as high-gain IEEE type AC4 excitation systems [56]. Each smaller machine is connected to a main bus by a transformer and a short transmission line. Only the smaller machines can be equipped with PSS units. All generators are equipped with a governor. The governor models are fourth and fifth order. Table 2 shows the generation of each machine in the system.

Generator	Generation (MW)
1	12,500
2	4,500
3	2,000
4	1,600
5	10,300
6	1,250
7	6,700
8	1,200
9	2,500
10	14,000
11	700
12	10,600
13	2,469
14	12,500
15	1,000
16	700
17	3,200

Table 2. Output of each generator (operating point A).

The system in Figure 26 also contains a 500 kV HVDC transmission line between areas NW2 and SC1. The dynamics of this line are not modeled for the simulations shown in this thesis. The DC line is modeled as a positive load at NW2 and as a negative load at SC1.

Five interarea modes in the 0.3 to 0.9 Hz range are present in the test system. These modes have machines in given areas swinging against those in other areas. One mode is at 0.37 Hz and has machines in areas A, P, and SC1 swinging against the remaining machines. A lightly-damped mode near 0.65 Hz has generators in area C swinging against the rest of the system, especially area A. The third interarea mode is at 0.72 Hz and has generators in areas C, P, and SC1 swinging together against the other areas. The

remaining two interarea modes are at 0.80 and 0.90 Hz. Machines in areas A, NW1, and NW2 swing together at the 0.80 Hz mode, and generators in area SC1 swing against those in areas A and P at the 0.90 Hz mode. The 0.80 Hz mode is difficult to excite and is relatively well damped. The 0.90 Hz mode is an unstable mode as it is slightly negatively damped. In addition to the five interarea modes, each smaller generator in the test system has its own local mode. These local modes are in the 1 to 2 Hz range.

In order to investigate the effectiveness of the proposed control schemes under different operating conditions, a second operating point is used. This operating point is shown in Figure 27, and is called operating point B. Operating points A and B differ in structure, line impedances, loading conditions, and generator operating conditions. As can be seen from Figures 26 and 27, the lines between areas C-M and A-U are removed at operating point B. When going from operating condition A to B, the power outputs of generators 4 and 10 are decreased by 20% and 3%, respectively, and the generation of machines 1, 2, 3, 12, 14, 15, and 16 are increased by 10%, 10%, 20%, 13%, 27%, 50%, and 42%, respectively. The loads at areas A, C, M, SC1, and SC2 are increased by 9%, 4%, 66%, 9%, and 11%, respectively. The impedances of the lines connecting generators 2, 3, 4, and

15 to the system are increased by 100%, 43%, 50%, and 50%. Also, the impedances of the lines between areas C-NW1 and P-NW1 are doubled.

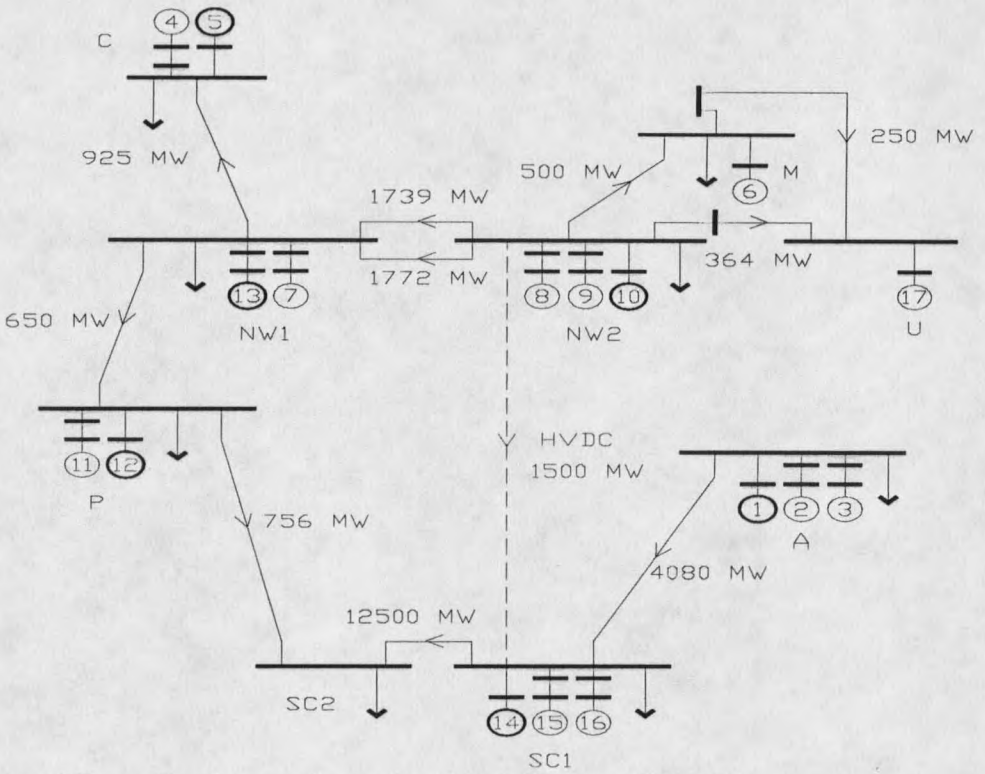

Figure 27. Test system (operating point B).

Both operating points of the test system are simulated using version 1 of the Extended Transient Midterm Stability Package (ETMSP). This standard simulation package was developed through the Electric Power Research Institute. Load-flow and the swing data files used to simulate the system using ETMSP are contained in Appendix C. These files contain all information about the test system, and the data files follow the format described in [57].

Implementation of PSS Units in the Test System

In this section a description of how PSS units are implemented in the test system is given. The design process for the application of PSS units on four machines in the system is described in detail. Both adaptive and conventional PSS units are designed. The adaptive ones use the decentralized scheme developed in Chapter 2. The conventional units are used as a comparison for the adaptive ones.

Before the design and implementation of the two different control schemes are discussed, general issues concerning PSS units are addressed. These include how a unit is applied to a generator, why the control action from a PSS is limited, criteria for choosing an effective feedback signal, and criterion for choosing which machines should have a PSS unit.

On all synchronous generators an excitation voltage must be applied to the rotor circuit so that a rotating magnetic field is provided to the stator. On standard generators the excitation voltage source is termed the exciter. An exciter typically has a feedback loop around it used to maintain the terminal voltage of the generator at a reference point. The PSS unit is a second feedback loop on the generator that is added to the input of the exciter. Typically, the PSS feedback signal is added to the generator's terminal reference voltage.

Figure 28 shows how a general PSS unit is applied to a generator. A PSS feedback signal is measured from the system. The signal is then band-pass filtered to remove any very low or high frequency components; the filter is termed a low-pass washout filter. The signal is filtered because the objective of the PSS unit is to dampen electromechanical oscillations which are in the 0.2 to 3.0 Hz range. It is desired that the controller have little effect on frequencies outside this range. The control action from the PSS unit is limited between ±0.1 per unit before it is added to the terminal reference voltage.

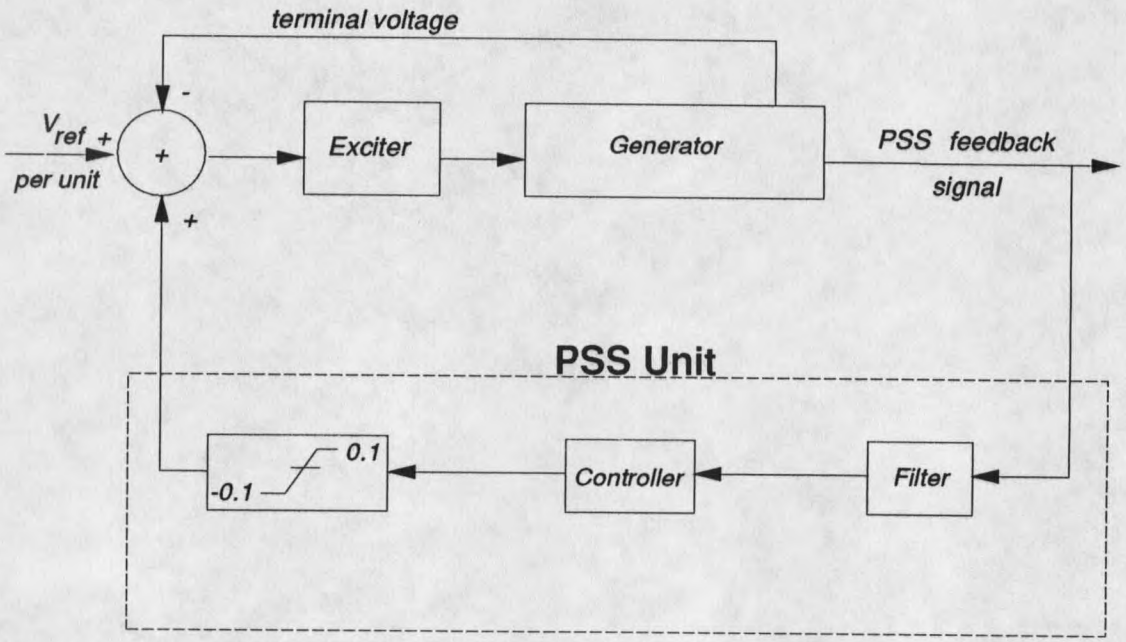

Figure 28. Implementation of a general PSS unit.

Limiting the PSS control signal to ±0.1 per unit prevents the stabilizer from interfering with the exciter during fast transients. When a fault occurs in the network

near a machine, often the exciter voltage must be immediately changed by a large factor so that the machine is not unnecessarily tripped off line. These fast transients are not due to electromechanical oscillations; therefore, the PSS signal is limited so that it does not interfere with the exciter operation during fast transients. The filter also helps prevent the PSS from interacting with the fast transients. Limiting the PSS signal also helps prevent the stabilizer from driving the exciter into saturation.

The ability of a PSS unit to add damping to a given electromechanical mode is dependent on the magnitude of the transfer-function residue for that mode at a given operating point. The larger a residue, the more the associated eigenvalue can be moved with a given feedback gain (see [58]). It is well known that a transfer-function residue is made up of controllability and observability factors. From state-space control theory, it is known that if a system is either uncontrollable or unobservable, then certain system eigenvalues cannot be moved [59]. The eigenvalues that cannot be moved are the ones that have residues of zero. This phenomena can also be viewed as a pole-zero cancellation. Looking at the transfer-function residues as controllability and observability factors is the basis for choosing a feedback signal. It is also used to determine which generators in the test system are to be equipped with

PSS units.

Any number of signals can be used for feedback with a PSS unit. Two common signals that have proven to be effective are rotor speed-error and accelerating power. Speed-error is the rotational speed of the rotor minus its synchronous speed, while accelerating power is the difference between the mechanical power turning the rotor and the electrical power out of the generator.

The objective of the PSS unit is to dampen both local and interarea modes. It is well known that the accelerating power of a generator has a relatively large residue for the local mode of that machine compared to interarea-mode residues. Since speed-error is proportional to the integral of accelerating power, it has larger interarea-mode residues. This is because the interarea modes are at lower frequencies then the local modes, and the integration operation tends to increase the residues of terms with smaller eigenvalues. Therefore, better damping of the interarea modes can be expected using a signal proportional to speed-error. The feedback signal used for all the PSS units in the test system is a signal proportional to speed-error. Speed-error is not directly used because it is not directly measurable in ETMSP. Therefore, it is obtained by integrating accelerating power (accelerating power is directly measurable in ETMSP).

Figure 28 shows how a general PSS unit is implemented on a generator. Now the question is which machines should be equipped with PSS units. To dampen a local mode, a PSS unit should be placed on the machine associated with that local mode. To dampen interarea modes, a machine that strongly participates in that mode should be equipped with a PSS. The amount a generator participates in a given interarea mode is proportional to the magnitude of the transfer-function residue for that mode. Therefore, generators that have large transfer-function residues for interarea modes are equipped with PSS units.

To determine which machines in the 17 machine test system are to have PSS units, the Prony identification method of Chapter 3 is used. An identification analysis is carried out for each of the smaller detailed machines in the system to determine which ones have large residues for interarea modes. The analysis is done at operating point A. Based on this analysis, the generators that are chosen to be equipped with stabilizers are 2, 3, 4, and 15. Generator 4 is equipped with a PSS because it has a relatively large residue for the 0.65 Hz and 0.72 Hz modes. Machines 2 and 3 are chosen as these have large residues for the 0.37, 0.65, 0.72, and the 0.90 Hz modes. Generator 15 is equipped with a stabilizer because it has a large residue for the 0.90 Hz mode. The 0.80 Hz mode is so widely spread over the system, none of the machines have relatively large

residues at this mode.

Decentralized Adaptive Controllers

The adaptive PSS units are implemented on the four generators using the decentralized adaptive scheme developed in Chapter 2. Figure 29 shows how an adaptive stabilizer is applied to a given generator in the test system. The accelerating power is measured and integrated to obtain a signal proportional to speed-error. Instead of actually integrating accelerating power, it is operated on by a very large time-constant block. This is done to avoid any integration "windup" which can cause numerical problems. With frequencies above 0.1 Hz, the large time-constant transfer function behaves like an integrator. The speed-error signal is low-pass washout filtered with the following Laplace-domain transfer function:

$$FILTER = \left(\frac{s}{s+0.2\pi}\right)\left(\frac{f_2}{s+f_2}\right) \tag{4.1}$$

After the speed-error signal is filtered, it is sampled by the adaptive controller. The adaptive controller calculates the control signal which is limited between ± 0.1 per unit before it is added to the reference voltage.

Two considerations must be taken into account when choosing a sampling rate for the discrete-time adaptive PSS unit. First, the rate must be greater than the Nyquist rate. Since electromechanical modes are below 3 Hz, the sampling rate must be greater than 6 Hz. Second, the rate

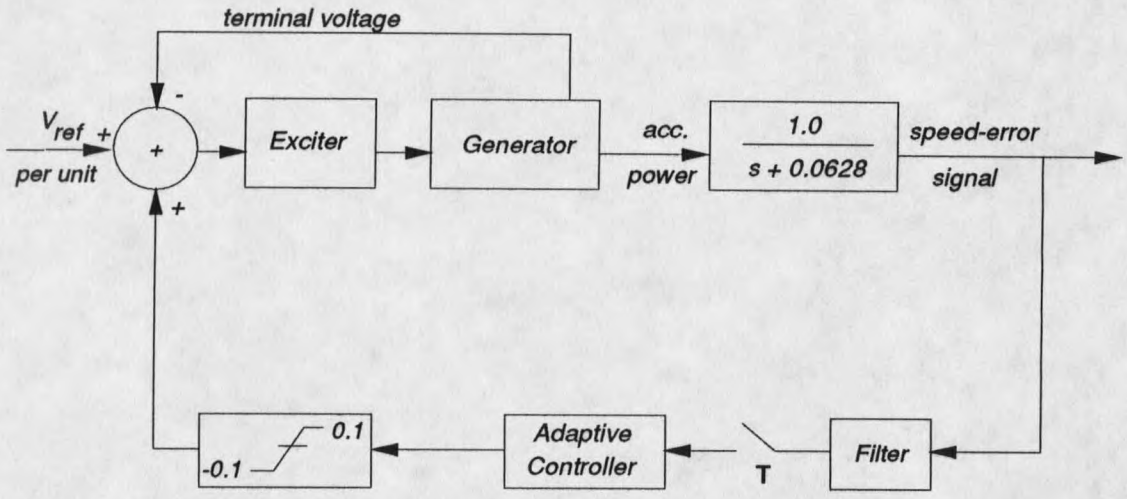

Figure 29. An adaptive PSS used in the test system.

must not be so fast as to cause numerical errors in the discrete-time controller. As the sampling rate increases, the discrete-time eigenvalues move closer together which is known to cause sensitivities in the discrete-time difference equations. With the simulation results in Chapter 5 sampling rates of 10 Hz and 16.67 Hz are used.

The choice of the high-end corner of the low-pass washout filter (i.e., f_2 in (4.1)) is also important. In many cases f_2 would have to be chosen to help prevent aliasing, but with the feedback configuration in Figure 29 aliasing is not a likely problem. This is because of the integrator block before the filter. The integrator acts as a low-pass filter. For the simulation cases in Chapter 5 where the sample rate is 10 Hz, the high-end corner is chosen to be 20 Hz (i.e., $f_2 = 20(2\pi)$ rad/sec.).

In many situations it is possible that a speed signal could be directly measured. This would allow the integration block in Figure 29 to be removed. Then f_2 must be chosen to be at least half the sampling rate to help prevent aliasing. This situation is simulated in Chapter 5 by choosing an 8 Hz corner when the sampling rate is 16.67 Hz (i.e., $f_2 = 8(2\pi)$ rad/sec.).

Criterion for Controller Communication. In theory the decentralized adaptive control scheme of Chapter 2 requires that all controllers communicate their control actions in order to guarantee global stability. Example 1 of Chapter 2 demonstrated that communication can mean the difference between stability and instability when the interconnections between subsystems are strong. But, example 4 showed that if subsystem interconnections are weak, little is actually gained from using communication. The magnitude of subsystem interconnections is the criterion used to determine the interconnection setup between the four adaptive PSS units in the test system. One way of measuring subsystem interconnections is the magnitude of transfer-function residues between the input of one generator and the output of other generators.

The criterion used to judge if communication is needed between two generators is the following: if the largest transfer-function residue between the two generators is of the same order of magnitude as the largest residue at one

of the generators, then communication is used between the controllers of the two generators. This test can be stated in a mathematical form: communication is not required between generators i and j if the following conditions are satisfied:

$$R_{ji} < \frac{R_{ii}}{10}, \qquad R_{ij} < \frac{R_{jj}}{10} \tag{4.2}$$

where R_{ii} is the magnitude of the largest transfer-function residue at generator i, R_{ij} is the magnitude of the largest residue from generator i to generator j, and R_{jj} and R_{ji} are the similar for generator j. Only electromechanical mode residues are considered. As before, the residues are obtained using the Prony identification method for system operating point A.

Consider generators 2 and 3. Table 3 shows the magnitude of the transfer-function residues for the input at the exciter of generator 2 and the output being the speed-error at generator 2 in one case and at generator 3 in a second case. Table 4 shows the same for generator 3. As expected, the largest residue magnitude at generator 3 is for that machine's local mode and is 21. The largest residue from generator 2 to 3 is 9.1 and is also for machine 3's local mode. These residues do not satisfy the test of (4.2); also, the largest residue from machine 3 to 2 does not satisfy the test. Therefore, communication is required between generators 2 and 3.

Output at	Residue Magnitudes for given modes						
	Interarea					Gen 3's local 1.62 Hz	Gen 2's local 1.68 Hz
	0.37 Hz	0.65 Hz	0.71 Hz	0.80 Hz	0.90 Hz		
Gen 2	5.6	0.94	0.63	0.25	1.1	3.6	43.0
Gen 3	2.0	0.44	0.20	0.20	0.50	9.1	0.0

Table 3. Residue magnitudes with input at generator 2.

Output at	Residue Magnitudes for given modes						
	Interarea					Gen 3's local 1.62 Hz	Gen 2's local 1.67 Hz
	0.37 Hz	0.65 Hz	0.71 Hz	0.80 Hz	0.90 Hz		
Gen 2	1.8	0.33	0.20	0.30	0.41	8.3	0.0
Gen 3	0.90	0.14	0.11	0.0	0.20	21.0	0.0

Table 4. Residue magnitudes with input at generator 3.

Note that the residues for all of the interarea modes satisfy the communication test for generators 2 and 3. This occurs because in most cases a given generator has a much larger residue for its own local mode than any of the interarea modes. Similar tests between all combinations of the four machines reveals that communication is only needed between generators 2 and 3. The others are spaced far enough apart in the network so that they do not interact at the local modes. As expected, the residue magnitudes between generators at the interarea modes are much less than the residue magnitude of the local-mode at a given generator.

Conventional Controllers

In order to judge the performance of the adaptive PSS units, conventional units are used as a comparison. The design method for the conventional stabilizers used here is unique in that it is based on a linear system obtained using the Prony identification technique of Chapter 3. Although the design method is unique, the resulting controller is in the form of a standard PSS unit.

Figure 30 shows how the conventional PSS units are applied to generators in the test system. As in the adaptive case, the accelerating power is integrated to obtain a signal proportional to the rotor's speed-error. The integration is done using a large time-constant transfer function to avoid integration windup. The speed-error signal is then low-pass washout filtered. With most conventional designs the filter coefficients are pre-chosen based on restricting the feedback to a specified frequency band. With the design method described here, the filter coefficients are chosen as part of the design. This allows additional freedom in the design. The filter is

$$FILTER = \left(\frac{s}{s+f_1}\right)\left(\frac{f_2}{s+f_2}\right) \qquad (4.3a)$$

where

$$f_1 > 0.2\pi, \quad f_2 < 40\pi \qquad (4.3b)$$

Conditions (4.3b) assures the feedback is limited to an allowable maximum bandwidth, but at the same time, (4.3b)

allows the designer to choose the filter coefficients to help enhance system damping. The feedback gain and lead-lag coefficients (i.e., the K, a's and b's in Figure 30) are chosen to enhance damping of electromechanical modes.

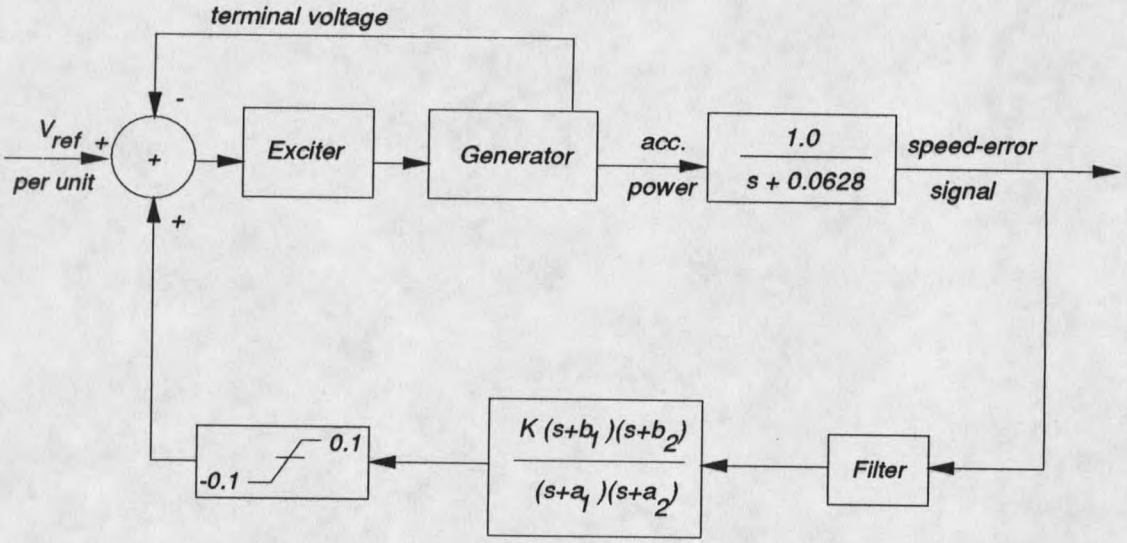

Figure 30. A conventional PSS used in the test system.

The design of a stabilizer at a given generator involves three steps. First, a reduced-order model of the system is identified at the generator using the Prony identification method. The model is obtained by probing the exciter where the PSS is to be connected and recording the signal that is proportional to the generator's rotor speed-error as the output. Second, a root-locus design method based on the identified model is used to choose the PSS coefficients and gain. The coefficients are chosen to make the loci move to the left as they depart their open-loop poles (departure angles of 180°). The gain is increased

until the damping ratio of the closed-loop poles no longer increases. Third, the gain and phase margins of the linear model with the stabilizer as a feedback is checked to make sure the design is reasonably robust.

A sequential decentralized technique is used to implement more than one PSS unit. With this technique the PSS units are designed and applied to their generators one at a time. The stabilizer at the first generator is designed and applied to the generator while the other PSS units are not applied. Then a model is identified for the second PSS unit and that unit is designed and applied to the system. The model for the third PSS unit is then obtained, and it is designed and applied to its generator. The process is continued until all PSS units are applied to the system. The conventional PSS units are designed for the test system in the following order: generators 4, 2, 15, and 3.

It is important that the design of a PSS unit is based on an accurate reduced-order model of the system. As discussed in Chapter 3, the choice of the probing signal is critical to obtaining as accurate model. The amplitude of the signal must be small enough so as not to force the system to significantly swing into nonlinear regions. The frequency content of the probing signal must contain the frequency range of the system. The probing signal and its frequency content used in the design of the conventional PSS units in the test system are shown in Figure 31. By